The Pennsylvania State University

The Graduate School

Department of Physics

BLACK HOLE COALESCENCE:

THE CLOSE LIMIT

A Thesis in

Physics

by

Gaurav Khanna

Submitted in Partial Fulfillment
of the Requirements
for the Degree of

Doctor of Philosophy

August 2000

We approve the thesis of Gaurav Khanna.

	Date of Signature
Jorge Pullin Associate Professor of Physics Thesis Advisor Chair of Committee	
Douglas Arnold Professor of Mathematics	
Pablo Laguna Associate Professor of Astronomy & Astrophysics	
Lee Smolin Professor of Physics	
Jayanth R. Banavar Professor of Physics Head of the Department of Physics	

Abstract

In this work we consider the problem of the coalescence of two black holes by modelling the collision as a perturbation of the final stationary black hole spacetime.

We first consider the slow inspiral of two spinless, equal mass black holes as a perturbation of Schwarzchild and Kerr spacetimes. We obtain estimates for the radiated energy, angular momentum and waveforms for the gravitational waves produced in such a collision. Toward this aim, we show how the perturbative functions (Zerilli and Teukolsky) can be calculated from the information about the initial perturbations of the metric and extrinsic curvature. We express different physical quantities in terms of these perturbative functions. We also compare and discuss the validity of the two approximations (Schwarzchild, Kerr) in this context. Lastly, we consider the inspiral of two spinning equal mass black holes.

Table of Contents

List of Figures

Acknowledgments

I am most grateful and indebted to my advisor, Jorge Pullin and also to Pablo Laguna for their constant guidance, patience, and encouragement. I am also very thankful for the financial support which they have provided to me over the years. I was supported by NSF grants PHY-9800973 and PHY-9423950.

I thank my other committee members for their insightful commentary on my work. I also thank Daniel Cartin, John Baker, Chris Beetle, Sameer Gupta, Joe Berry and several other fellow graduate students for help and useful discussions. I thank my family and friends for their good wishes and blessings. Lastly, I thank the Pennsylvania State University for making all this possible.

Chapter 1

Introduction

In the next few years, several interferometric gravitational wave observatories (the LIGO project in the US, the VIRGO and GEO projects in Europe and the TAMA project in Japan [4]) may be capable of detecting gravitational waves. This could have revolutionary implications for astronomy since it constitutes a new form of "light" with which to observe the universe, a form that is better correlated with the bulk motions of matter and is very hard to shield or distort. Attributes of a good source of gravitational waves include strong gravitational fields and high velocities, so black hole processes are a natural source to consider. It is astrophysically plausible that black holes form binary associations with other objects, including other black holes [5]. Due to the loss of energy by the emission of gravitational radiation, the separation and period of the binary orbits would decrease. If the binary consists of two black holes, the inspiral would end with a rapid strong field merger that has the potential to be a powerful source of detectable gravitational waves [6].

The whole process of inspiral generates gravitational radiation, but in the early large-separation stages the radiation is relatively weak and is reasonably well described by Newtonian gravity theory and Post-Newtonian extensions of it [7]. It is only the final strong field merger that could in principle produce a powerful burst of gravitational

waves. But at this point only one parameter of the burst is reliably known. The characteristic frequency of the waves is inversely proportional to the mass of the final black hole formed, and works out to be on the order of 10^3 Hz for a $10\,M_\odot$ hole, a typical expected mass of a "stellar" sized hole. For supermassive holes of mass $\geq 10^6 M_\odot$ typical of galactic nuclei, the waves would be less than 1 Hz. The maximum sensitivity of the next generation of gravitational wave detectors occurs at frequency around 100 Hz and the detectors will be ideally suited to waves from a black hole with mass of several hundred $M_\odot$. Some recent observations[8] offer indirect evidence that black holes in this range may exist. If they do not, then the detection of the collision of black holes may require the deployment of space-based detectors[9] sensitive to the low frequency waves produced by supermassive holes.

General relativity, Einstein's theory of gravity, sets the dynamics of space-time via a set of nonlinear partial differential equations of such complexity that analytic solutions have been limited to two classes: solutions of high symmetry, or solutions based on approximation techniques, such as linearized weak field theory. The study of Einstein's equations on computers has been viewed as the key to finding more general asymmetric strong field solutions and it was natural for this key to be be applied to black hole collisions. Black holes are incontrovertibly strong field regions, but single isolated black holes are stationary solutions of Einstein's theory, and the simplifying symmetry of time independence allows for closed form well-understood solutions [2]. Collisions of black holes, on the other hand, are necessarily nonstationary as well as being crucially strong-field events. It is known that the collision will result in a single final black hole and in the generation of gravitational waves carrying off some of the mass energy originally

associated with the holes. But this is all that is known with certainty. The nature of the merging of the horizons, in the general collision, is not even qualitatively understood.

A reasonably complete understanding awaits progress in numerical relativity, and the wait has been longer than anticipated. The solution of general black hole collisions on computers has proved to be remarkably difficult. There is, however, a class of cases in which reliable answers are available. If the collision is a 'head-on' collision along a straight line, then there is rotational symmetry about the line of the collision. Though the collision is still highly dynamic and nonlinear, the simplifications afforded by this symmetry reduce the computational demands sufficiently that the collision could successfully be simulated even in the mid 1970's, and run with good reliability in the mid 1990's[3]. The simplification of head-on collisions, however, masks some of the physics of the most interesting types of collisions, the fully three dimensional collisions at the end point of the inspiral of a mutually orbiting pair of black holes.

Interest in these issues justifies approximation methods that can help, even slightly, to close some of the wide open questions. We take such an approach here. We offer an estimate of the gravitational radiation generated during the late stage of inspiral of two equal mass black holes. Our method involves a number of assumptions and limitations that constrain its applicability and reliability, but for all its shortcomings it is one step towards a complete understanding. For two different reasons, we focus here on the collision of roughly equal mass holes. The first is that the power radiated from the collision of holes of masses $m_1 \leq m_2$ scales as $(m_1/m_2)^2$, at least in the case that m_1 is significantly smaller than m_2. The strain produced in a detector will then scale as m_1/m_2, and collisions of equal mass holes will be the most detectable. The second reason is

that computations in the case $m_1 \ll m_2$ can be done by treating the smaller mass as a particle perturbing the spacetime of the larger. The equations that describe perturbations are linear, and hence relatively easily dealt with in general. The techniques of calculation were worked out in the 1970s and resulted in the Regge-Wheeler and Zerilli equations [10, 11] for perturbations of Schwarzschild (nonrotating) black holes, and in the Teukolsky [12] equation for perturbations of Kerr (rotating) black holes.

The approximation method we use, the "close limit," [15] takes advantage of the property of a black hole horizon. Late in the merger of the binary the single horizon of the final black hole engulfs the entire binary. All the complex structure of the binary will be inside that final horizon, and cannot influence spacetime outside the horizon. It is only what is outside the horizon that can generate gravitational waves that can be detected by distant observers. Since the ultimate fate of the merger is a stationary black hole, it follows that sufficiently late in the merger what is outside the hole will be a perturbation of the final stationary hole. Thus the gravitational waves generated during the latest stage of inspiral can be computed using the techniques of perturbations of black hole spacetimes, with the Zerilli, Regge-Wheeler, and Teukolsky equations.

There are reasons beyond speculation to believe that close limit evolutions give useful answers. Numerical relativity results are available for axisymmetric head-on collisions[3]. These represent evolution of a number of initial value solutions, in particular the closed form solution due to Misner[17], containing a single parameter representing the initial separation of equal mass holes in units of the mass of the spacetime (in $c = G = 1$ units). This separation index defines a parameterized family of initial value solutions. Choices of this parameter can be made corresponding to large or small

initial separation. When numerical relativity and close limit results are compared it is seen that agreement is excellent for small initial separations, and is surprisingly good even when the initial configuration is not close enough for a horizon to engulf the entire binary[18, 19]. Arguments can be made also, that the gravitational waves calculated in the late stage of inspiral are not highly sensitive to details of initial data. Particularly interesting in this regard is work by Abrahams and Cook[20].

In the past several years the close limit method has been extensively studied for head-on collisions of boosted and spinning holes and compared with the results of numerical relativity. Most notably, second order perturbation theory has been developed for the close limit method[21]. In this process of comparison much has been learned about the strengths and limitations of the close limit method, with the goal of applying the method to problems that cannot yet be handled with numerical relativity. The present work represents the first example of this. We report here the results of the application of the close limit method for the three dimensional problem of the late stage inspiral of two black holes.

We will use the close limit method for the initial data families constructed by the Bowen and York [22] method and the associated "punctures" families [23]. It is known that these families possess an artificial radiation content when one considers black holes that are close, but such content is also known to be moderate [24]. An important advantage of these methods is that they are typically the starting point for numerical relativity, and thus close limit evolution of these starting points can be compared with the numerical evolution of these same initial data when such evolutions become available. The most important disadvantage, for our purposes, is that the Bowen-York family does not

include the Kerr solution, the solution for a rotating hole. This precludes finding a family of initial value solutions that goes, in the limit of small initial separation, to a Kerr black hole. With Bowen-York initial value solutions, then, we cannot consider a collision that will result in a rapidly rotating hole. Rather, we limit our attention to collisions involving a modest amount of total angular momentum and consider the angular momentum as well as the initial separation to be a perturbation of a nonrotating final hole. It it should also be mentioned that currently fashionable astrophysical scenarios suggest that the individual holes might not carry a significant amount of spin [5] in realistic black hole collisions.

The organization of this work is as follows: I only include research that has been done either entirely by me, or in close collaboration with others (J. Baker, C. O. Nicasio, H.-P. Nollert, R. Gleiser, R. Price, J. Pullin). All needed background has been referred to, at appropriate places. In the next chapter, the main part of this work, we set up the perturbative formalism and the close-slow approximation method to solve the nonspinning black hole inspiral problem. In chapter 3 we consider the effects of individual spin on binary black hole inspiral, and we summarize and discuss future directions in chapter 4. The appendix explains the technique we use to calculate initial data for the Teukolsky function.

Chapter 2

Inspiralling black holes in the close limit

In this chapter we will consider the inspiral of two equal mass, non-spinning holes, to form a final rotating black hole. We first review the method for obtaining the initial data and describe the approximations involved. In the following two sections we discuss how to set up the perturbative formalism geared towards evolution. Since the collisions have net angular momentum we will evolve them *both* as a perturbation of a rotating and a non-rotating black hole. The comparison of both approaches is given in the subsequent section and we will see that insight is gained by treating the problem in two different ways. We end this chapter, with a discussion of the results in terms of waveforms and radiated energies and we describe a puzzle in the calculation of the angular momentum radiated.

Some parts of this work were independently done by John Baker [48].

2.1 Initial data

To evolve a spacetime in general relativity, one needs to provide initial data, a 3-geometry g_{ab} and an extrinsic curvature K_{ab}, that solve Einstein's equations on some starting hypersurface (i.e., at some starting time). For two black holes, this is an easy task if the holes are far apart, since one can superpose the solutions for two individual holes ignoring their interactions. When the black holes are close on the initial

hypersurface, the astrophysically correct initial data is the solution corresponding to what would have evolved during the binary inspiral, but such an evolution cannot be computed with present day techniques. One must therefore use a somewhat artificial initial data solution that is a best guess at a representation of close black holes. The need for such a guess is one of the sources of uncertainty in our result.

2.1.1 Summary of the Bowen–York construction:

The initial value equations for general relativity are,

$$\nabla^a (K_{ab} - g_{ab} K) = 0 \tag{2.1}$$

$$^3R - K_{ab}K^{ab} + K^2 = 0 \tag{2.2}$$

where g_{ab} is the spatial metric, K_{ab} is the extrinsic curvature and ^3R is the scalar curvature of the three metric. If we propose a 3-metric that is conformally flat $g_{ab} = \phi^4 \widehat{g}_{ab}$, with $\widehat{g}_{ab}$ a flat metric, and ϕ^4 the conformal factor, and we use a decomposition of the extrinsic curvature $K_{ab} = \phi^{-2}\widehat{K}_{ab}$, and assume maximal slicing $K^a_a = 0$, the constraints become,

$$\widehat{\nabla}^a \widehat{K}_{ab} = 0 \tag{2.3}$$

$$\widehat{\nabla}^2 \phi = -\frac{1}{8}\phi^{-7}\widehat{K}_{ab}\widehat{K}^{ab} \ , \tag{2.4}$$

where $\widehat{\nabla}$ is a flat-space covariant derivative.

To solve the momentum constraint, we start with a solution that represents a single hole with linear momentum P [25],

$$\hat{K}^{\rm one}_{ab} = \frac{3}{2r^2}\left[2P_{(a}n_{b)} - (\delta_{ab} - n_a n_b)P^c n_c\right] \ . \tag{2.5}$$

In this expression for the conformally related extrinsic curvature at some point x^a, the quantity n_b is a unit vector, in the "base" flat space with metric $\hat{g}_{ab}$, directed from a point representing the location of the hole to the point x^a. The symbol r represents the distance, in the flat base space, from the point of the hole to x^a. It is straightforward to show that the solution of the Hamiltonian constraint corresponding to eq. (5) corresponds to a spacetime with ADM momentum P_a.

The next step is to modify this to represent holes centered at $x = \pm L/2$ in the conformally flat metric. Since the momentum constraint is linear, we can simply add two expressions of the above form,

$$\widehat{K}^{\rm two}_{ab} = \widehat{K}^{\rm one}_{ab}\left(x \to x - L/2, P_y = P\right) + \widehat{K}^{\rm one}_{ab}\left(x \to x + L/2, P_y = -P\right) \ . \tag{2.6}$$

We will choose in further expressions to use a polar coordinate system in the flat space determined by $\hat{g}_{ab}$ centered in the mid-point separating the two holes and label the polar coordinates as (R, θ, ϕ). So R will be the distance in the flat space from the midpoint between the holes.

To solve the Hamiltonian constraint 2.4, we introduce an approximation, (the slow approximation) which we will show is enough for our purposes. In fact, in this approximation the solution for the conformal factor turns out to be the familiar Misner

[17] solution if one chooses the topology of the slice to have a single asymptotically flat region, or the Brill–Lindquist [26] solution if there are three asymptotically flat regions.

2.1.2 The slow approximation

We assume that the black holes are initially close, and that the initial momentum P is small. We denote by $\vec{n}^+$ and $\vec{n}^-$ the normal vectors corresponding, respectively, to the one hole solutions at $x = +L/2$ and at $x = -L/2$, and we define R to be the distance to a field point, in the flat conformal space, from the point midway between the holes. For large R, the normal vectors $\vec{n}^+$ and $\vec{n}^-$ almost cancel. More specifically $\vec{n}^+ = -\vec{n}^- + O(L/R)$. A consequence of this is that the total initial $\hat{K}^{ab}$ is first order in L/R, and its $(R, \theta, \varphi$ coordinate basis) components can be written as

$$\hat{K}_{ab} = \frac{3PL}{8R^3} \begin{bmatrix} 8\sin^2\theta \sin 2\varphi & 0 & 8R\sin^2\theta \\ 0 & R^2(-5+\cos 2\theta)\sin 2\varphi & -2R^2 \sin 2\varphi \sin 2\theta \\ 8R\sin^2\theta & -2R^2 \sin 2\varphi \sin 2\theta & R^2 \sin^2\theta \sin 2\varphi(1+3\cos 2\theta) \end{bmatrix} . \tag{2.7}$$

This solution for $\hat{K}_{ab}$ is first order, both in P and L. Thus the source term in the Hamiltonian constraint is quadratic in P. If we choose to find a solution to the conformal factor to first order in P (which should give us a good approximation in the case of slowly moving holes), we can ignore this quadratic source term. So now, the Hamiltonian constraint looks like the one for zero momentum, which is simply the Laplace equation. A well known solution to this, is the Misner solution [17]. This solution, is characterized by a parameter μ_0 which describes the separation of the two

throats. We can relate this parameter to the conformal distance L in the following way [3],

$$L/M = \frac{\coth\mu_0}{2\Sigma_1} \qquad\qquad \Sigma_1 \equiv \sum_{n=1} \frac{1}{\sinh n\mu_0} \,. \tag{2.8}$$

To clarify: in the slow approximation we are considering, the data we use in our simulations consists of the extrinsic curvature proposed by Bowen and York and the conformal factor due to Misner. This might appear as odd, since the conformal factor of Misner is "symmetrized" through the throats and the extrinsic curvature due to Bowen and York is not. What we do is not inconsistent, it is just a different (and perhaps from a certain point of view less natural) choice of boundary conditions for the fields. In practice, in the close limit and to first order in perturbation theory, the conformal factor of Misner differs from that of Brill and Lindquist by a numerical factor that can be absorbed in the definition of the separation of the holes [27].

Some readers may be disturbed by the slow approximation, since in the computation of certain quantities, for instance the ADM mass, the higher order terms in the expansion in terms of the momentum are crucial. We have already discussed this in detail in previous head-on simulations [28]. The bottomline is that to get an accurate estimate of the ADM mass for high values of the momentum one indeed needs a full solution of the Hamiltonian constraint and not a "slow approximation" solution. For the values of the separations and the momenta we will consider in this work ($a < 0.5$) the ADM mass computed with the slow approximation and the one computed with the full solution differ by less than 10% so we will ignore this difference.

We must now map the coordinates of the initial value solution to the coordinates for the Schwarzschild/Kerr (in the vanishing spin limit) background. To do this, we interpret the R as the isotropic radial coordinate of a Schwarzschild spacetime, and we relate it to the usual Schwarzschild radial coordinate r by $R = (\sqrt{r}+\sqrt{r-2M})^2/4$. From this we arrive at the following expression for the components of the extrinsic curvature,

$$K_{ab} = \frac{3PL}{8r^3}\begin{bmatrix} \frac{8\sin^2\theta\sin 2\varphi}{1-2M/r} & 0 & \frac{8r\sin^2\theta}{\sqrt{1-2M/r}} \\ 0 & r^2(-5+\cos 2\theta)\sin 2\varphi & -2r^2\sin 2\varphi\sin 2\theta \\ \frac{8r\sin^2\theta}{\sqrt{1-2M/r}} & -2r^2\sin 2\varphi\sin 2\theta & r^2\sin^2\theta\sin 2\varphi(1+3\cos 2\theta) \end{bmatrix} . \tag{2.9}$$

Here we have used the fact that

$$\phi^2 \approx \phi^2_{\rm Mis} \approx \phi^2_{\rm Schw} = r/R = \frac{1}{\sqrt{1-2M/r}}\frac{dr}{dR} . \tag{2.10}$$

2.2 The close limit as a perturbation of a Schwarzschild hole

In this work we will evolve the initial data we just constructed using the perturbative evolution equations for linearized first order perturbations: the Zerilli equation in the case of a Schwarzschild background and the Teukolsky equation in the case of a Kerr background. We need to construct the initial data for these equations in terms of the metric and extrinsic curvature we discussed above. In this section we discuss the setup of initial data and evolution of the problem as a perturbation of a Schwarzschild black hole, using the Zerilli–Regge–Wheeler formalism.

2.2.1 Setting up the initial data for the Zerilli function

Given the three metric and the extrinsic curvature, one can explicitly construct the zeroth and first order term of a power series expansion in a fiducial time variable t of the space-time metric. From this expression one can read off the appropriate coefficients of the multipolar expansion of the metric in the Regge–Wheeler [10] notation. The only nonvanishing perturbations at $t = 0$ are,

$$\begin{aligned} H_2[\ell = 2, m = \pm 2] &= K[\ell = 2, m = \pm 2] = \sqrt{\frac{6\pi}{5}} \frac{8ML^2}{\sqrt{r}(\sqrt{r} + \sqrt{r - 2M})^5} \\ H_2[\ell = 2, m = 0] &= K[\ell = 2, m = 0] = -2\sqrt{\frac{\pi}{5}} \frac{8ML^2}{\sqrt{r}(\sqrt{r} + \sqrt{r - 2M})^5} \end{aligned} \tag{2.11}$$

We compute the time derivative of these quantities, using the extrinsic curvature K_{ij} obtained in the last section. The nonvanishing ones are,

$$\begin{aligned} \frac{\partial H_2[\ell = 2, m = -2]}{\partial t} &= -i24\sqrt{\frac{\pi}{30}} PL \frac{\sqrt{r - 2M}}{r^3\sqrt{r}} \\ \frac{\partial H_2[\ell = 2, m = 2]}{\partial t} &= -\frac{\partial H_2[\ell = 2, m = -2]}{\partial t} \\ \frac{\partial K[\ell = 2, m = -2]}{\partial t} &= i\sqrt{30\pi} PL \frac{\sqrt{r - 2M}}{r^3\sqrt{r}} \\ \frac{\partial K[\ell = 2, m = 2]}{\partial t} &= -\frac{\partial K[\ell = 2, m = -2]}{\partial t} \\ \frac{\partial G[\ell = 2, m = -2]}{\partial t} &= i\sqrt{\frac{6\pi}{5}} PL \frac{\sqrt{r - 2M}}{r^3\sqrt{r}} \\ \frac{\partial G[\ell = 2, m = 2]}{\partial t} &= -\frac{\partial G[\ell = 2, m = -2]}{\partial t} \end{aligned} \tag{2.12}$$

where i is the imaginary unit. (Here we are using the standard conventions for the spherical harmonics. Notice that the $m = 2$ and $m = -2$ perturbations are individually

complex, but when they are added to give the total perturbation the resulting function of t, r, θ and φ is real, as of course it must be.

We also have an odd parity contribution,

$$\frac{\partial\ {}^{\rm odd}h_1[\ell=1,m=0]}{\partial t} = 8\sqrt{3\pi}\frac{PL}{r^2}. \tag{2.13}$$

This perturbation represents the difference between the Kerr solution that represents the rotating space-time and the Schwarzschild background used in the perturbative approach. To first order it decouples from all other perturbations, and in fact is unchanging in time, corresponding to the conservation of angular momentum to first order in the perturbations. The change over time in the quantity induced by *second* order perturbations, will be discussed below in connection with the radiation of angular momentum.

The Zerilli function is defined by (see for instance [30]),

$$\begin{aligned}\psi_{(\ell,m)} &= \frac{2r(r-2M)}{\ell(\ell+1)(\lambda r+3M)}\left[H_{2(\ell,m)} - r\frac{\partial K_{(\ell,m)}}{\partial r} - \frac{r-3M}{r-2M}K_{(\ell,m)}\right] \\ &\quad + \frac{r^2}{\lambda r+3M}\left[K_{(\ell,m)} + (r-2M)\left(\frac{\partial G_{(\ell,m)}}{\partial r} - \frac{2}{r^2}h_{1(\ell,m)}\right)\right].\end{aligned} \tag{2.14}$$

Therefore, for $t=0$ we have

$$\psi_{(2,m)}(0,r) = \frac{r(r-2M)}{3(2r+3M)}\left[H_{2(2,m)}(0,r) - r\frac{\partial K_{(2,m)}(0,r)}{\partial r}\right] + \frac{r}{3}K_{(2,2)}(0,r). \tag{2.15}$$

and

$$\dot{\psi}_{(2,m)}(0,r) = \frac{r(r-2M)}{3(2r+3M)}\left[\dot{H}_{2(2,m)}(0,r) - r\frac{\partial \dot{K}_{(2,m)}(0,r)}{\partial r} + 3r\frac{\partial \dot{G}_{(2,m)}}{\partial r}\right] + \frac{r}{3}\dot{K}_{(2,2)}(0,r). \tag{2.16}$$

After some simplifications we have the initial data for the Zerilli function,

$$\psi_{(2,2)}(0,r) = 4\sqrt{\frac{2\pi}{15}}ML^2\frac{r\,(7\sqrt{r}+5\sqrt{r-2M})}{(2r+3M)(\sqrt{r}+\sqrt{r-2M})^5} \tag{2.17}$$

and

$$\dot{\psi}_{(2,2)}(0,r) = -\frac{i\sqrt{30\pi}}{5}PL\frac{(4r+3M)\sqrt{r-2M}}{r^{5/2}(2r+3M)} \tag{2.18}$$

and the Zerilli function for $(\ell = 2, m = -2)$ is the complex conjugate of $\psi_{(2,2)}(t,r)$. The initial data for the $\ell = 2, m = 0$ Zerilli function is

$$\psi_{(2,0)}(0,r) = -\frac{8}{3}\sqrt{\frac{\pi}{5}}\frac{ML^2r\,(7\sqrt{r}+5\sqrt{r-2M})}{(2r+3M)(\sqrt{r}+\sqrt{r-2M})^5} \tag{2.19}$$

$$\dot{\psi}_{(2,0)}(0,r) = 0. \tag{2.20}$$

2.2.2 Evolution of the Zerilli function and computation of physical quantities

Given the Cauchy data from the last section, the time evolution is obtained from the Zerilli equation [30],

$$-\frac{\partial^2 \psi_{(\ell,m)}}{\partial t^2} + \frac{\partial^2 \psi_{(\ell,m)}}{\partial r_*^2} + V(r_*)\psi_{(\ell,m)} = 0, \tag{2.21}$$

where $V(r_*)$ is the (m-independent) Zerilli potential,

$$V(r_*) = 2\left(1 - \frac{2M}{r}\right)\frac{\lambda^2 r^2\left[(\lambda+1)r + 3M\right] + 9M^2(\lambda r + M)}{r^3(\lambda r + 3M)^2}\,, \tag{2.22}$$

where $\lambda = (\ell-1)(\ell+2)/2$ and $r_* = r + 2M\ln(r/2M - 1)$.

We need to establish a convenient formula for the radiated energy, similar to that present in [31] but applied to the non-axisymmetric case. We start from the expression of the radiated energy computed via the Landau–Lifshitz pseudo-tensor following the notation and derivations of [31],

$$\frac{d\text{Power}}{d\Omega} = \lim_{r\to\infty}\frac{1}{16\pi r^2}\left[\left(\frac{\dot{h}_{\theta\phi}}{\sin\theta}\right)^2 + \frac{1}{4}\left(\dot{h}_{\theta\theta} - \frac{1}{\sin^2\theta}\dot{h}_{\phi\phi}\right)^2\right], \tag{2.23}$$

and translating to the Regge–Wheeler notation and integrating on solid angles we get,

$$\text{Power} = \frac{3}{16\pi}\left[2\left|\dot{\psi}_{(2,0)}\right|^2 + 4\left|\dot{\psi}_{(2,2)}\right|^2\right] \tag{2.24}$$

and one can obtain the radiated energy integrating over time. The power naturally comes out in units of the mass of the background spacetime.

To compute the radiated angular momentum one could also start by considering the Landau–Lifshitz pseudo-tensor and construct and asymptotic expression for angular momentum flux. This approach was pursued, for instance, in [32] to compute expressions for the radiation of angular momentum in terms of multipoles. An alternative approach is to simply compute the change in the angular momentum of the spacetime, which we characterize to linear order in perturbation theory through the function,

$$r^2\ {}^{\rm odd}h_{0,r}\,(r,t) - 2r\ {}^{\rm odd}h_0(r,t)r^2 - \ {}^{\rm odd}h_{1,t}\,(r,t). \tag{2.25}$$

This is a first order gauge invariant if ${}^{\rm odd}h_0$, and ${}^{\rm odd}h_1$ are first order perturbations. Moreover, for $\ell = 1, m = 0$, this gauge invariant is constant, equal to $4\sqrt{3\pi}J$, where J is the total angular momentum, if the perturbations are axially symmetric.

If we look at second order perturbations we find

$$\frac{\partial}{\partial t}\left[r^2\ {}^{\rm odd}h_{0,r}\,(r,t) - 2r\ {}^{\rm odd}h_0(r,t) - r^2\ {}^{\rm odd}h_{1,t}\,(r,t)\right] = \mathcal{S}_{\rm Jdot} \tag{2.26}$$

where $\mathcal{S}_{\rm Jdot}$ is a 'source', quadratic in first order perturbations.

Therefore the change in angular momentum, due to radiation may be obtained by integrating $\mathcal{S}_{\rm Jdot}$ for all t (or from $t = 0$ to $t = \infty$, it makes no difference), in the limit $r \to \infty$. After several simplifications and cancelling terms that result from integration

by parts, we end up with

$$\Delta J = \frac{3i}{4\pi} \lim_{r\to\infty} \int_0^\infty \left[\psi_{(2,-2)}(r,t) \frac{\partial \psi_{(2,2)}(r,t)}{\partial t} - \psi_{(2,2)}(r,t) \frac{\partial \psi_{(2,-2)}(r,t)}{\partial t} \right] dt \quad (2.27)$$

We have checked by explicit substitution that this form coincides with the results from the flux formulas of Thorne [32]. It reassures our confidence in the consistency of the Regge–Wheeler–Zerilli perturbative formalism to notice that the changes to second order are in accordance with the first order flux.

2.3 Evolution as a perturbation of a Kerr black hole

To treat the problem as a perturbation of a Kerr black hole we need to set up initial data and evolve the Teukolsky equation. The formalism for setting up initial data in terms of Cauchy metric data was developed in [33], we only give a brief sketch here and refer the reader to the appendix for further details.

The relevant Weyl scalar for gravitational radiation is

$$\psi_4 = -C_{\alpha\beta\gamma\delta} n^\alpha \overline{m}^\beta n^\gamma \overline{m}^\delta, \quad (2.28)$$

since it is directly related to outgoing gravitational waves. We can rewrite this as

$$-\psi_4 = R_{ijkl} n^i \overline{m}^j n^k \overline{m}^l + 4R_{0jkl} n^{[0} \overline{m}^{j]} n^k \overline{m}^l + 4R_{0j0l} n^{[0} \overline{m}^{j]} n^{[0} \overline{m}^{l]}, \quad (2.29)$$

which in turn can be written in terms of hypersurface quantities g_{ij} and K_{ij}. For the last term in this expression, we can use vacuum Einstein equations to eliminate terms

that have time derivatives of K_{ij}. Also, we are interested merely in the first order perturbations of this scalar. Putting all this together, the final result for the first order expansion of the Weyl scalar is ([33] or see appendix),

$$\begin{aligned} -\psi_4 &= \left[R_{ijkl} + 2K_{i[k}K_{l]j}\right]_{(1)} n^i \overline{m}^j n^k \overline{m}^l - 8N_{(0)} \left[K_{j[k,l]} + {}^{p}_{j[k}K_{l]p}\right]_{(1)} n^{[0}\overline{m}^{j]} n^k \overline{m}^l \\ &\quad + 4N_{(0)}^2 \left[R_{jl} - K_{jp}K^p_l + KK_{jl}\right]_{(1)} n^{[0}\overline{m}^{j]} n^{[0}\overline{m}^{l]} \end{aligned} \tag{2.30}$$

where $N_{(0)} = (g^{tt}_{\text{kerr}})^{-1/2}$ is the zeroth order lapse, $n^i, \overline{m}^j$ are two of the null vectors of the (zeroth order) tetrad, Latin indices run from 1 to 3, and the brackets are computed to only first order (zeroth order excluded).

This expression can be used, to obtain the time derivative of the Weyl scalar too. We simply replace the first order quantities above by their time derivatives (which can be obtained via the Einstein equations).

In our treatment, the extrinsic curvature and the metric, from the last section, shall be treated as a perturbation of the corresponding Kerr hypersurface quantities. Since we attempt calculations only to first order in PL (which we identify with Ma, where M is the mass of the background Kerr black hole and a its angular momentum parameter), the Kerr 3-metric is (in this approximation) conformally flat. Hence we justify using the Bowen York recipe for constructing initial data for the inspiral problem.

2.3.1 Initial Data for the Teukolsky function:

Using the methodology and expressions we just discussed, the initial data for the Teukolsky function, $\Psi = \rho^{-4}\psi_4$, where $\rho = -1/(r - ia\cos\theta)$, is:

For the azimuthal modes, $m = \pm 2$

$$-\frac{\Psi}{\sqrt{2\pi}} = \left[\frac{3rM(2M-r)L^2}{32R^2(2R+M)} \pm i\frac{3}{8}Ma\left(1-\frac{2M}{r}\right)^{\frac{3}{2}}\right](\cos\theta \pm 1)^2 \tag{2.31}$$

$$-\frac{\dot{\Psi}}{\sqrt{2\pi}} = -\left[\frac{3(2M-r)M^2L^2}{16rR^2(2R+M)} \pm i\frac{3Ma}{16r^2}(2r-21M)\left(1-\frac{2M}{r}\right)^{\frac{3}{2}}\right](\cos\theta \pm 1)^2 \tag{2.32}$$

And for the azimuthal mode, $m = 0$

$$-\frac{\Psi}{\sqrt{2\pi}} = \frac{3rM(r-2M)L^2}{16R^2(2R+M)}\sin^2\theta \tag{2.33}$$

$$\dot{\Psi} = -\frac{2M}{r^2}\Psi \tag{2.34}$$

Here, R is the Schwarzschild isotropic radial coordinate.

2.3.2 Evolution of the Data using the Teukolsky equation

Given the Cauchy data from the last section, the time evolution is obtained from the Teukolsky equation [12],

$$\left\{\left[a^2\sin^2\theta - \frac{(r^2+a^2)^2}{\Delta}\right]\partial_{tt} - \frac{4Mar}{\Delta}\partial_{t\varphi} + 4\left[r + ia\cos\theta - \frac{M(r^2-a^2)}{\Delta}\right]\partial_t\right.$$
$$+\Delta^2\partial_r\left(\Delta^{-1}\partial_r\right) + \frac{1}{\sin\theta}\partial_\theta(\sin\theta\partial_\theta) + \left[\frac{1}{\sin^2\theta} - \frac{a^2}{\Delta}\right]\partial_{\varphi\varphi} \tag{2.35}$$
$$\left. -4\left[\frac{a(r-M)}{\Delta} + \frac{i\cos\theta}{\sin^2\theta}\right]\partial_\varphi - \left(4\cot^2\theta + 2\right)\right\}\Psi = 0, \tag{2.36}$$

where M is the mass of the black hole, a its angular momentum per unit mass, $\Sigma \equiv r^2 + a^2 \cos^2\theta$, and $\Delta \equiv r^2 - 2Mr + a^2$.

The radiated energy is given by [34],

$$\frac{dE}{dt} = \lim_{r\to\infty} \left\{ \frac{1}{4\pi r^6} \int_\Omega d\Omega \left| \int_{-\infty}^{t} d\tilde{t}\ \Psi(\tilde{t}, r, \theta, \varphi) \right|^2 \right\}, \quad d\Omega = \sin\theta\ d\vartheta\ d\varphi, \tag{2.37}$$

and the angular momentum carried away by the waves can be obtained from [34],

$$\frac{dJ_z}{dt} = -\lim_{r\to\infty} \left\{ \frac{1}{4\pi r^6} \mathrm{Re} \left[\int_\Omega d\Omega \left(\partial_\varphi \int_{-\infty}^{t} d\tilde{t}\ \Psi(\tilde{t}, r, \theta, \varphi) \right) \left(\int_{-\infty}^{t} dt' \int_{-\infty}^{t'} d\tilde{t}\ \overline{\Psi}(\tilde{t}, r, \theta, \varphi) \right) \right] \right\}. \tag{2.38}$$

2.4 Results of the evolutions

We have evolved the Zerilli and Teukolsky equations using codes that have already been tested in other situations [28], [35]. The waveforms that follow concern a collision of two black holes that were initially separated by a conformal distance of 0.91 and had an orbital angular momentum of 0.1 in units of ADM mass.

Let us turn now to the evaluation of the radiated energies and angular momentum. Figure 2.7 shows the radiated energy as a function of the initial angular momentum, for a fixed separation of the holes. The figure compares the Regge–Wheeler–Zerilli (Z) and Teukolsky (T) calculations. As expected, they differ for large values of the angular momentum, since the Teukolsky calculation contains terms higher than linear in the angular momentum. As we explained before, one is not keeping consistently these higher order terms so one cannot argue that the Teukolsky result is "better". A conservative

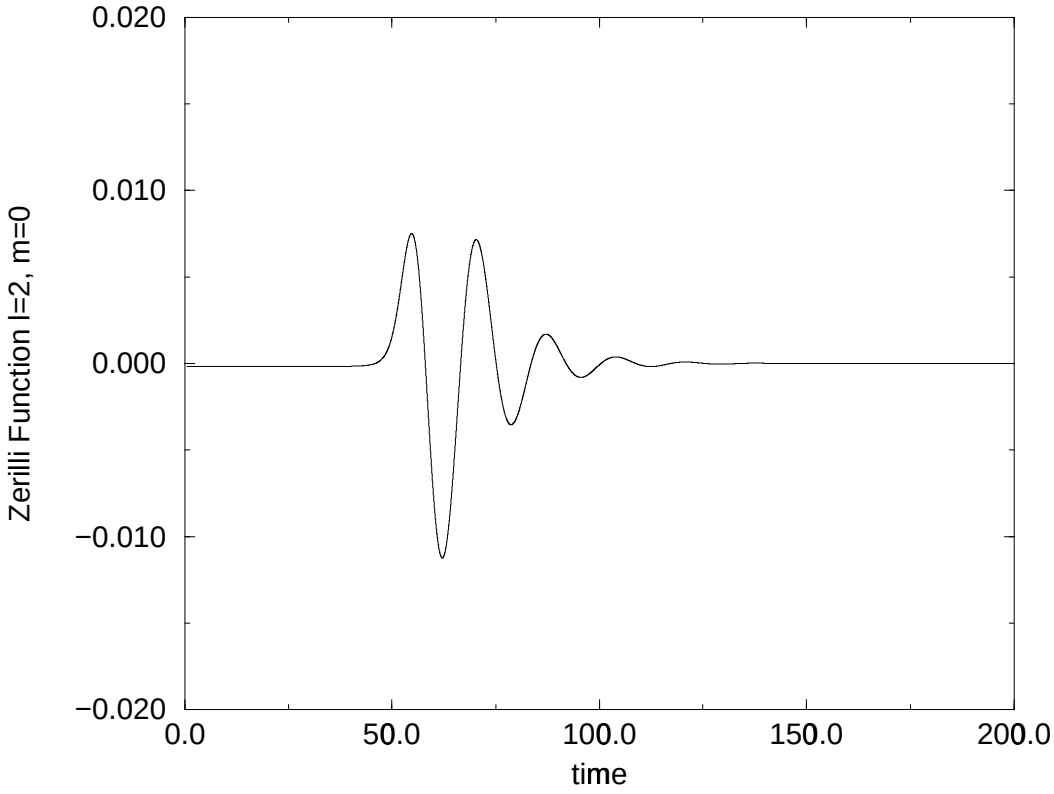

Fig. 2.1. This is the real part of the $l = 2$, $m = 0$ mode of the Zerilli function. The imaginary part is zero. All quantities are in units of ADM mass.

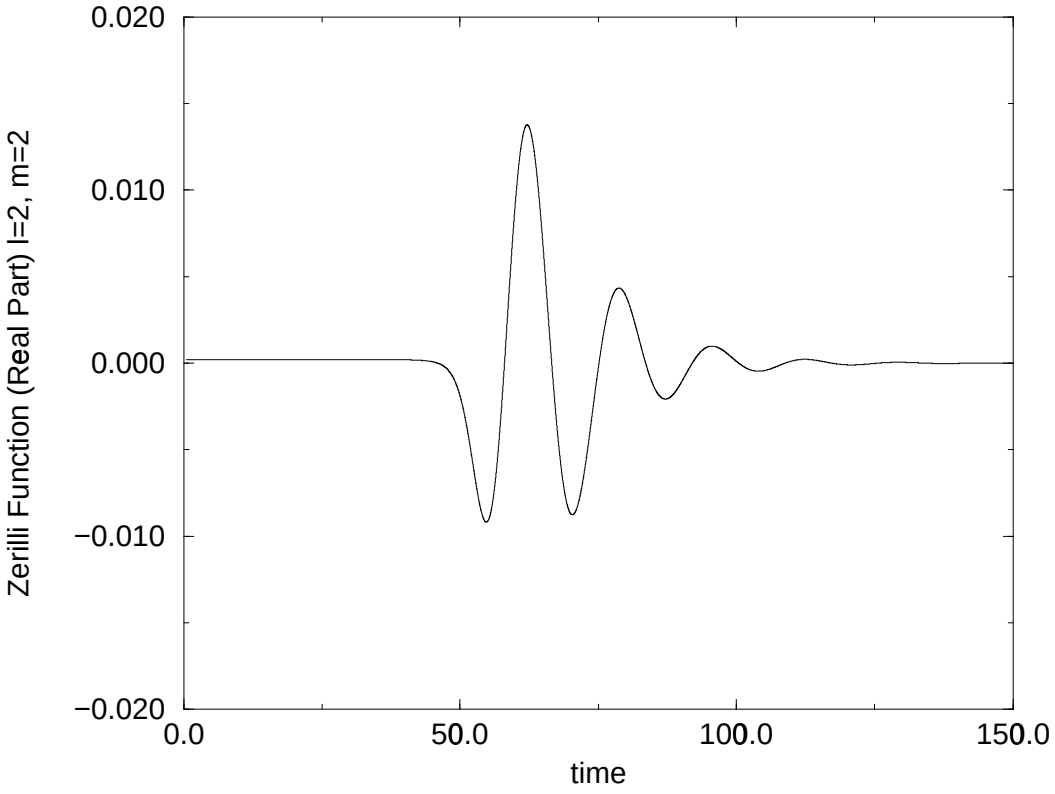

Fig. 2.2. This figure depicts the real part of the $l = 2$, $m = 2$ mode of the Zerilli function. The real part of the $l = 2$, $m = -2$ mode looks the same. All quantities are in units of ADM mass.

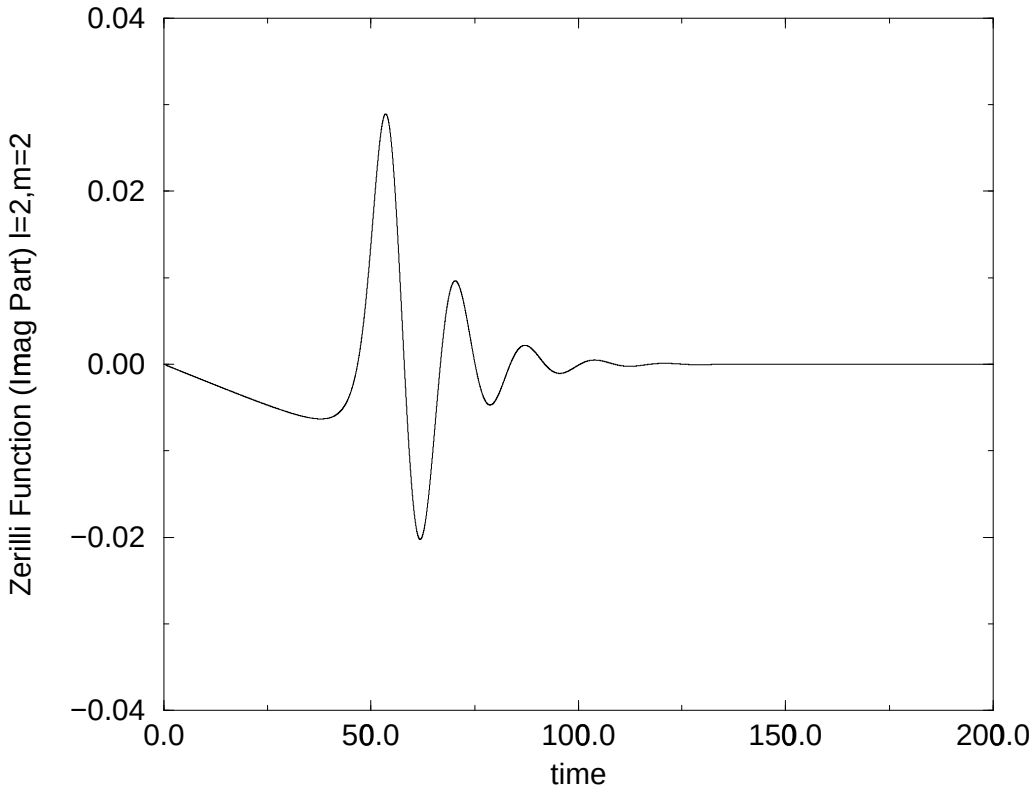

Fig. 2.3. The imaginary part of the $l = 2$, $m = 2$ mode of the Zerilli function. The imaginary part of the $l = 2$, $m = -2$ has an identical form, if multiplied by a -1. All quantities are in units of ADM mass.

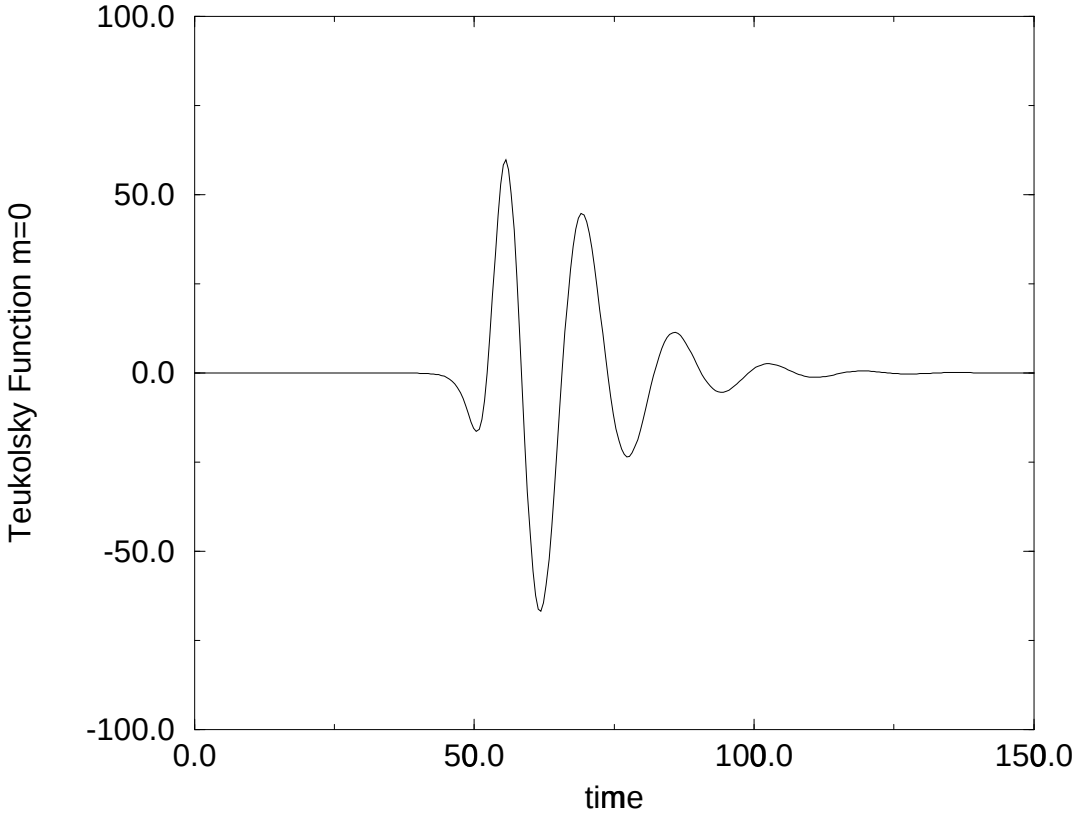

Fig. 2.4. This figure depicts the real part of the $m = 0$ mode of the Teukolsky function. The imaginary part of this mode is zero. All quantities are in units of ADM mass.

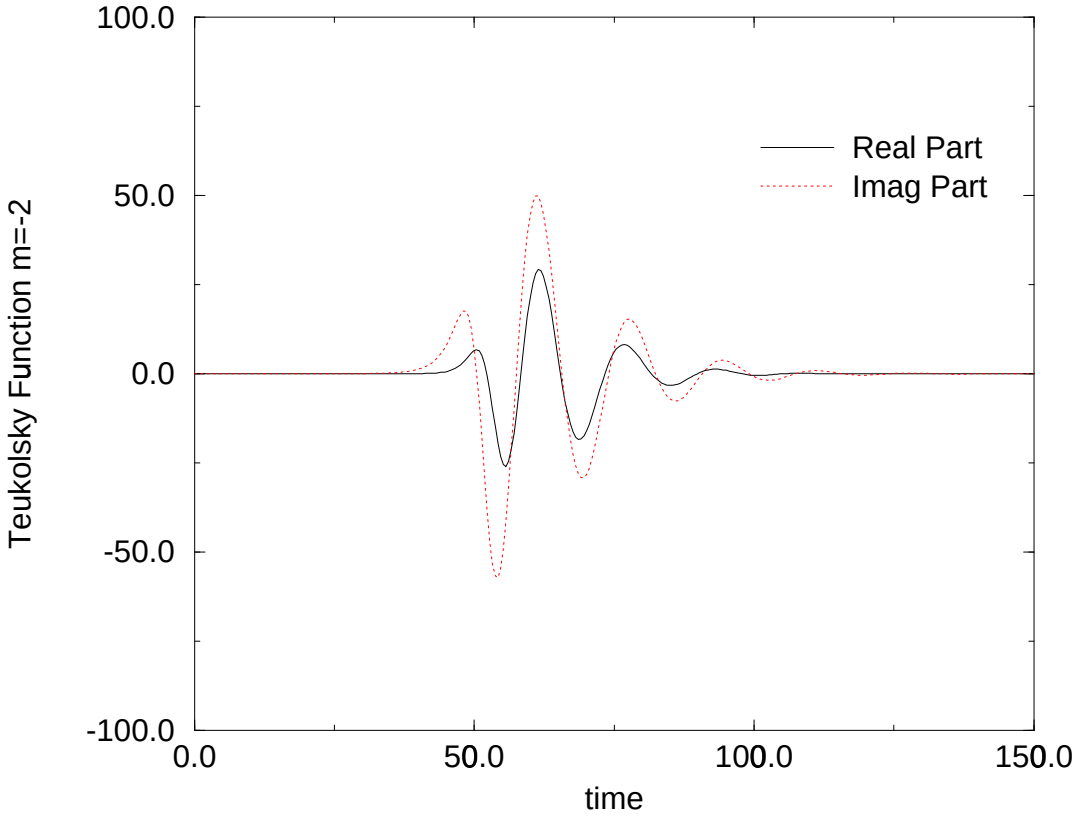

Fig. 2.5. This is the real and imaginary part of the $m = -2$ mode of the Teukolsky function. The real part is indicated by a solid line, while the imaginary part is depicted by a dotted line. All quantities are in units of ADM mass.

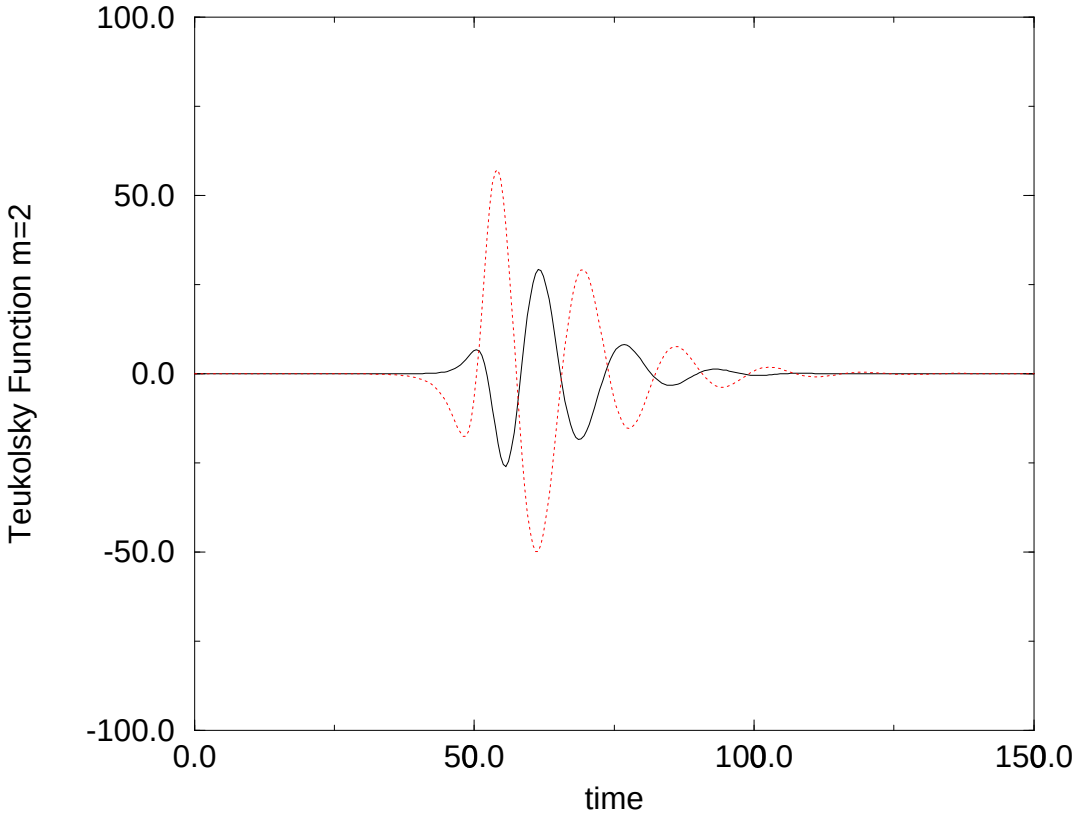

Fig. 2.6. This is the real and imaginary part of the $m = 2$ mode of the Teukolsky function. The real part is indicated by a solid line, while the imaginary part is depicted by a dotted line. All quantities are in units of ADM mass.

view that can be taken should be that both results disagree when higher order terms start to be important, and this gives us a rough measure of the error in the Zerilli calculation. We therefore conclude that for the separation in question, one should not trust first order perturbation theory beyond $a = 0.5$. One should stress that this view can be somewhat overconservative, our experience with explicit second order calculations for the head-on collisions [36, 37, 30] shows that one should include *all* second order terms to have a consistent formulation and a reliable set of "error bars". This is not accomplished by the first order Teukolsky formalism in this context. In this respect, second order Teukolsky results for this problem will be quite welcome [34]. The second order Zerilli calculations appear as quite prohibitive in complexity.

A remarkable aspect of figure 2.7 is that linear perturbation theory has a tendency to *overestimate* the radiated energies for large values of the perturbative parameter, at least from our experience with head-on collisions of non-boosted [18], boosted [28] and some preliminary unpublished results we have for spinning holes. This would suggest that, if the same behavior takes place for the inspiralling collisions, "reality" should lie below the curve corresponding to the Regge–Wheeler–Zerilli formalism (Z). This would indicate that the estimation obtained using the Teukolsky formalism is actually *worse* for the particular kind of collision under consideration. This is what we were alluding to when we warned in the introduction that it was not obvious that representing the spacetime as a perturbation of a non-rotating hole was a worse choice than of that of a Kerr hole.

We now turn to the evaluation of the radiated angular momentum. This is depicted in figure 2.8.

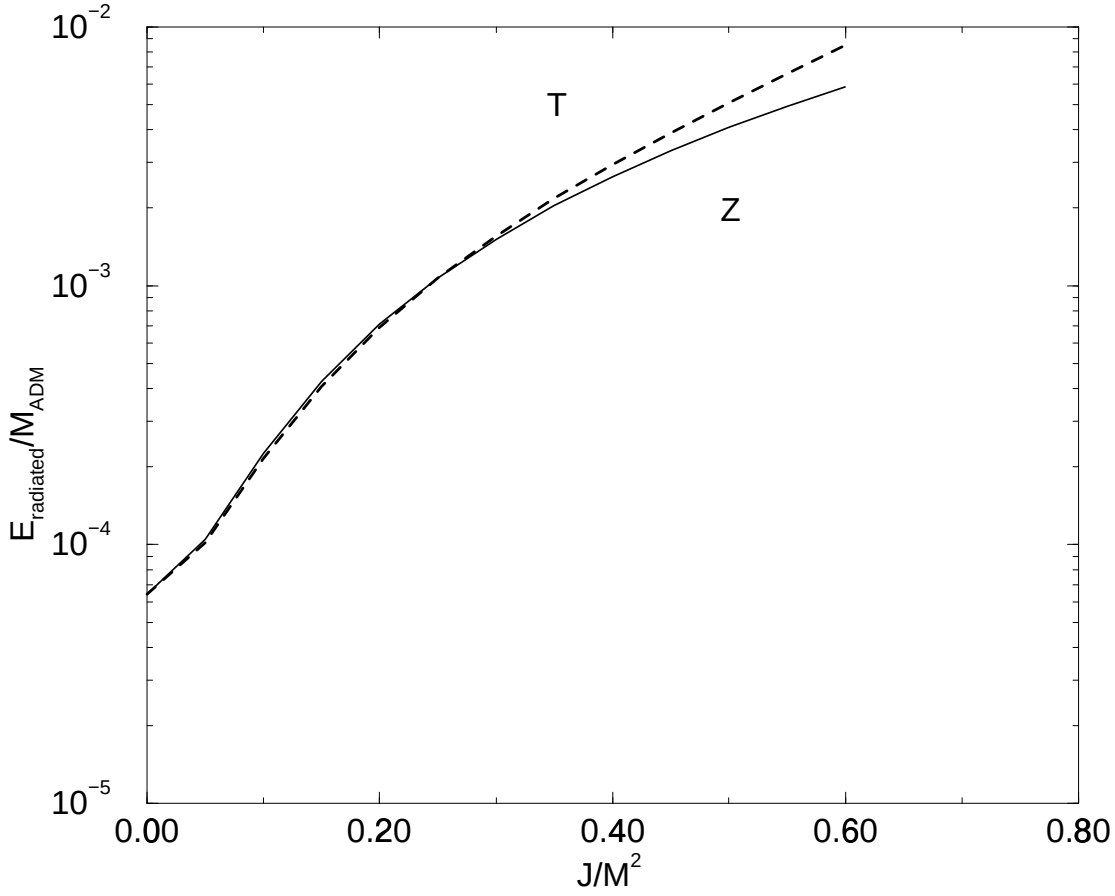

Fig. 2.7. The radiated energy in a non-head-on collision of two non-spinning black holes as a function of the total initial angular momentum, for a fixed conformal separation of 0.91 in ADM mass units. We depict the results of treating the problem as a perturbation of a non-rotating hole (Z) and a rotating hole (T). The agreement of both curves up to angular momenta of $a = 0.4 - 0.5$ gives confidence in the linear perturbative results. The "real data" very likely lies in a curve below the Zerilli (Z) curve, which allows us to roughly extrapolate the results to the extremal $a = 1$ case, where we see that still less than 1% of the mass of the system is radiated in the close limit.

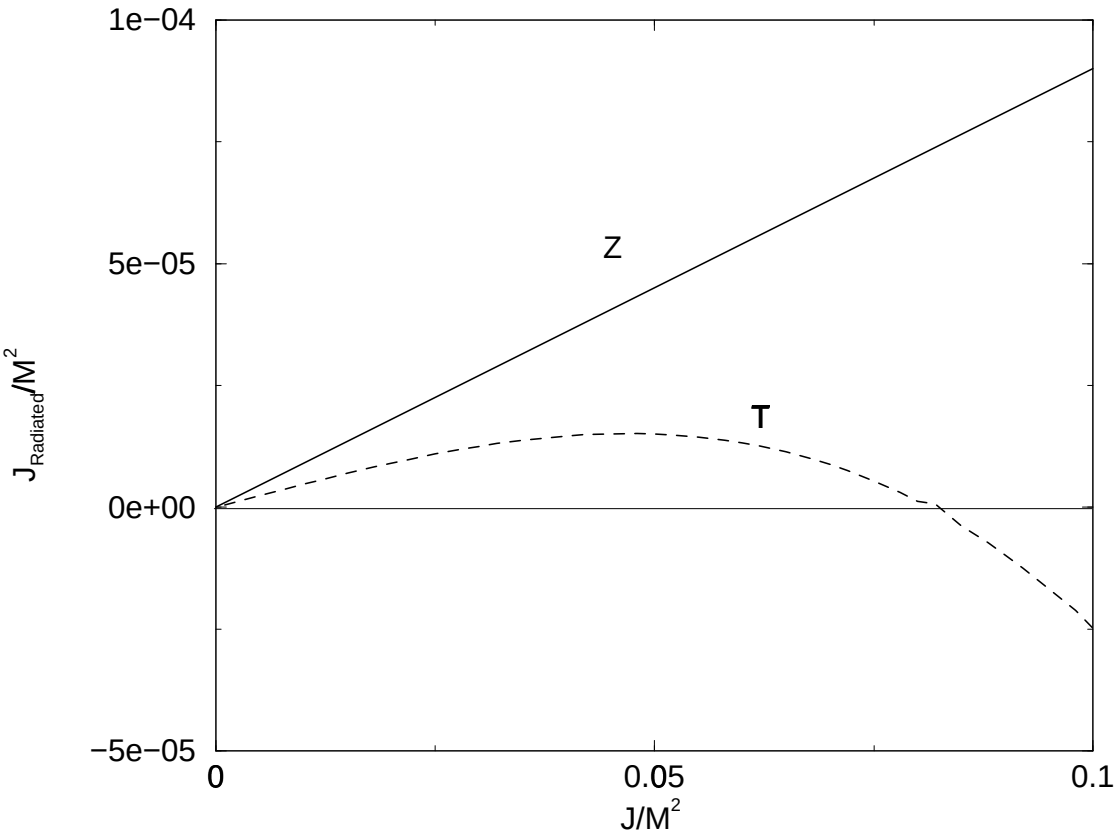

Fig. 2.8. Radiation of angular momentum. As can be seen, the Regge–Wheeler-Zerilli (Z) calculation of perturbations of a non-rotating hole disagrees with the Teukolsky (T) rotating black hole calculation. The radiated angular momentum is a more delicate quantity to compute than the energy and it appears that the potentially inconsistent higher order terms included in the rotating perturbation approach changes its value significantly. Overall we see the radiation is small. The Regge–Wheeler–Zerilli curve predicts less than 0.1% of the total angular momentum will be radiated, even in the extreme rotating case.

The two curves shown in 2.8 disagree significantly. They do not even agree for very small values of the angular momentum. We have checked that there is no numerical error: if in the Teukolsky evolution one keeps the initial data intact but "turns off" the a-dependent terms in the evolution equation, the RWZ straight line is reproduced. It should be noticed that the radiated angular momentum is a qualitatively different quantity insofar as its computation than the energy. The energy is roughly obtained by squaring and integrating the waveforms. The angular momentum depends on subtle phase differences. It is much more easy to disturb the calculation of the radiated angular momentum than that of the radiated energy. This, in particular, points out to the potential difficulty of estimating this kind of quantity in full numerical simulations, where phase lags in the waveforms due to grid stretching and other problems are well known. In our approach it appears that the potentially inconsistent higher order terms in the angular momentum we introduce when considering a rotating background are causing problems in the computation of radiated angular momentum. If one wishes to be ultra-conservative, one could simply conclude that both calculations only predict the correct result for zero angular momentum. Otherwise, one could conclude that for this family of initial data the Teukolsky approach really only works for non-rotating black holes, something suggested by the fact that the background spacetime is only recovered in the close limit with vanishing angular momentum. At the moment we can only say that the accurate computation of the radiated angular momentum for this problem is an open problem. It is likely that the RWZ estimate is correct, but we do not have "error bars" (even rough ones) to validate this prediction.

Chapter 3

Collision of spinning black holes

In the previous chapter, we analyzed the inspiral of two equal mass, non-spinning black holes. Here we will consider the collision of spinning holes. Since we are attempting a linear, first order perturbative calculation, it is sufficient to study the coalescence of two spinning holes with zero initial momentum. This is because, to obtain the results for the inspiral of spinning holes, one can simply do a linear superposition of these results with those from the last chapter.

However, the first order perturbative treatment imposes several restrictions on the physical scenarios we can treat. In addition to the close-slow limitations, we can only analyze easily cases in which the spins of the two black holes are equal and opposite. This happens because, to lowest order, the (perturbative) extrinsic curvature of a black hole with spin S and a conformal distance L from the origin is of order SL. Superposing another hole with parallel and equal spin and at $-L$ will yield a situation with zero perturbation in extrinsic curvature, which is not a case of interest.

So in the following, we shall present two cases that are exhaustive. *Case I*, when the two spins are equal and opposite and aligned along the common axis of the two holes. Specifically, we follow the set-up of the last chapter, and place the two holes at $x = \pm L/2$ and have their spins parallel and anti-parallel to the x-axis. *Case II*, when the two spins are equal and opposite and perpendicular to the common axis of the two holes.

Following the set-up of the previous chapter again, we place the two holes at $x = \pm L/2$ and have their spins parallel and anti-parallel to the y-axis.

The cases we consider in this chapter have no net angular momentum. So we expect Zerilli and Teukolsky formalisms to agree exactly (Kerr parameter $a = 0$). We, therefore report calculations and results from the Teukolsky formalism only. These cases have been considered in context of the Zerilli formalism by Hans-Peter Nollert [47].

3.1 Initial data – Case I

Following the Bowen–York construction as outlined in the first section of the previous chapter, and using the close-slow approximation, we arrive at the following expressions for the initial spatial metric and extrinsic curvature:

$$K_{ab} = \frac{3SL}{Rr^2}\begin{bmatrix} 0 & \frac{-2\sin\theta\sin 2\varphi}{\sqrt{1-2M/r}} & \frac{-2\sin\theta\sin 2\theta\cos^2\varphi}{\sqrt{1-2M/r}} \\ \frac{-2\sin\theta\sin 2\varphi}{\sqrt{1-2M/r}} & r\cos\theta\sin 2\varphi & r\sin\theta(\cos^2\theta\cos^2\varphi - \sin^2\varphi) \\ \frac{-2\sin\theta\sin 2\theta\cos^2\varphi}{\sqrt{1-2M/r}} & r\sin\theta(\cos^2\theta\cos^2\varphi - \sin^2\varphi) & -r\sin^2\theta\cos\theta\sin 2\varphi \end{bmatrix}. \tag{3.1}$$

The metric has a form, identical to the Misner solution [17].

3.1.1 Initial Data for the Teukolsky function – Case I:

Using the methodology and expressions we discussed in the last chapter, the initial data for the Teukolsky function, $\Psi = \rho^{-4}\psi_4$, where $\rho = -1/(r - ia\cos\theta)$, is:

For the azimuthal modes, $m = \pm 2$

$$-\frac{\Psi}{\sqrt{2\pi}} = -\frac{3}{4} i (\cos\theta \pm 1)^2 LS \frac{(r-2M)(-1+2\sqrt{1-\frac{2M}{r}})}{r(r(1+\sqrt{1-\frac{2M}{r}})-M)} \tag{3.2}$$

$$-\frac{\dot{\Psi}}{\sqrt{2\pi}} = -\frac{3}{4} i (\cos\theta \pm 1)^2 LS \frac{(r-2M)(-3r+8M+3(r-7M)\sqrt{1-\frac{2M}{r}})}{r^3(r(1+\sqrt{1-\frac{2M}{r}})-M)} \tag{3.3}$$

And for the azimuthal mode, $m = 0$

$$-\frac{\Psi}{\sqrt{2\pi}} = \frac{3}{2} i \sin^2\theta LS \frac{(r-2M)(-1+2\sqrt{1-\frac{2M}{r}})}{r(r(1+\sqrt{1-\frac{2M}{r}})-M)} \tag{3.4}$$

$$-\frac{\dot{\Psi}}{\sqrt{2\pi}} = \frac{3}{2} i \sin^2\theta LS \frac{(r-2M)(-3r+8M+3(r-7M)\sqrt{1-\frac{2M}{r}})}{r^3(r(1+\sqrt{1-\frac{2M}{r}})-M)} \tag{3.5}$$

To all these expressions, we also need to add metric contributions, that have the same form as the ones in the last chapter.

3.2 Initial data – Case II

Again, following the Bowen–York construction as outlined in the first section of the previous chapter, and using the close-slow approximation, we arrive at the following expressions for the initial spatial metric and extrinsic curvature:

$$K_{ab} = \frac{3SL}{Rr^2}\begin{bmatrix} \frac{2\cos\theta}{r-2M} & \frac{\sin\theta(4\cos^2\varphi-1)}{\sqrt{1-2M/r}} & \frac{-\sin 2\theta\sin\theta\sin 2\varphi}{\sqrt{1-2M/r}} \\ \frac{\sin\theta(4\cos^2\varphi-1)}{\sqrt{1-2M/r}} & -2r\cos\theta\cos^2\varphi & \frac{r}{2}\sin\theta(1+\cos^2\theta)\sin 2\varphi \\ \frac{-\sin 2\theta\sin\theta\sin 2\varphi}{\sqrt{1-2M/r}} & \frac{r}{2}\sin\theta(1+\cos^2\theta)\sin 2\varphi & -\frac{r}{2}\sin\theta\sin 2\theta\sin 2\varphi \end{bmatrix} . \tag{3.6}$$

The metric has form, identical to the Misner solution [17].

3.2.1 Initial Data for the Teukolsky function – Case II:

Using the methodology and expressions we discussed in the last chapter, the initial data for the Teukolsky function, $\Psi = \rho^{-4}\psi_4$, where $\rho = -1/(r - ia\cos\theta)$, is:

For the azimuthal modes, $m = \pm 2$

$$-\frac{\Psi}{\sqrt{2\pi}} = \mp\frac{3}{4}(\cos\theta \pm 1)^2 LS\frac{(r-2M)(-1+2\sqrt{1-\frac{2M}{r}})}{r(r(1+\sqrt{1-\frac{2M}{r}})-M)} \tag{3.7}$$

$$-\frac{\dot{\Psi}}{\sqrt{2\pi}} = \mp\frac{3}{4}(\cos\theta \pm 1)^2 LS\frac{(r-2M)(-3r+8M+3(r-7M)\sqrt{1-\frac{2M}{r}})}{r^3(r(1+\sqrt{1-\frac{2M}{r}})-M)} \tag{3.8}$$

And for the azimuthal mode, $m = 0$ the initial data are identically zero.

To all these expressions we need to add the metric contributions, that have a form identical to the one in the last chapter.

3.3 Evolution of the Data using the Teukolsky equation

Recall that, given the Cauchy data from the last section, the time evolution is obtained from the Teukolsky equation [12],

$$\left\{ \left[a^2 \sin^2\theta - \frac{(r^2+a^2)^2}{\Delta} \right] \partial_{tt} - \frac{4Mar}{\Delta}\partial_{t\varphi} + 4\left[r + ia\cos\theta - \frac{M(r^2-a^2)}{\Delta} \right] \partial_t \right.$$

$$+ \Delta^2 \partial_r \left(\Delta^{-1} \partial_r \right) + \frac{1}{\sin\theta}\partial_\theta \left(\sin\theta \partial_\theta \right) + \left[\frac{1}{\sin^2\theta} - \frac{a^2}{\Delta} \right] \partial_{\varphi\varphi} \tag{3.9}$$

$$\left. - 4\left[\frac{a(r-M)}{\Delta} + \frac{i\cos\theta}{\sin^2\theta} \right] \partial_\varphi - \left(4\cot^2\theta + 2 \right) \right\} \Psi = 0, \tag{3.10}$$

where M is the mass of the black hole, a its angular momentum per unit mass, $\Sigma \equiv r^2 + a^2\cos^2\theta$, and $\Delta \equiv r^2 - 2Mr + a^2$.

The radiated energy is given by [34],

$$\frac{dE}{dt} = \lim_{r\to\infty} \left\{ \frac{1}{4\pi r^6} \int_\Omega d\Omega \left| \int_{-\infty}^{t} d\tilde{t}\ \Psi(\tilde{t}, r, \theta, \varphi) \right|^2 \right\}, \quad d\Omega = \sin\theta\ d\vartheta\ d\varphi, \tag{3.11}$$

3.4 Results of the evolutions

In this section we show waveforms and plots for energy radiated from the collision of two spinning holes. Recall that the two holes have equal mass and equal and opposite spin, and we are considering two cases, *Case I* in which the spins are aligned along the common axis of the two holes, and *Case II* in which the two spins are perpendicular to the common axis of the two holes.

The waveforms that follow, are for a collision of two black holes that were initially separated by a conformal distance of 0.91 and had an individual spin of 0.1 in units of ADM mass.

Let us turn now to the evaluation of the radiated energies for these two cases. Figure 3.7 shows the radiated energy as a function of the initial spin, for a fixed separation of the holes. The first noteworthy thing is that the two curves, corresponding to *Case I* and *Case II* are very close to each other throughout. This indicates that the geometry of the initial configuration does not matter much as far as energy loss is concerned. The next important observation (by looking at the trend of the curves for large spin) is that, even for high values of the initial spin of the two holes this type of collision radiates less than 1% of its total mass. This means that inclusion of spin does *not* dramatically change our original estimate of a percent of the mass-energy being carried away by gravity waves in binary black hole inspiral.

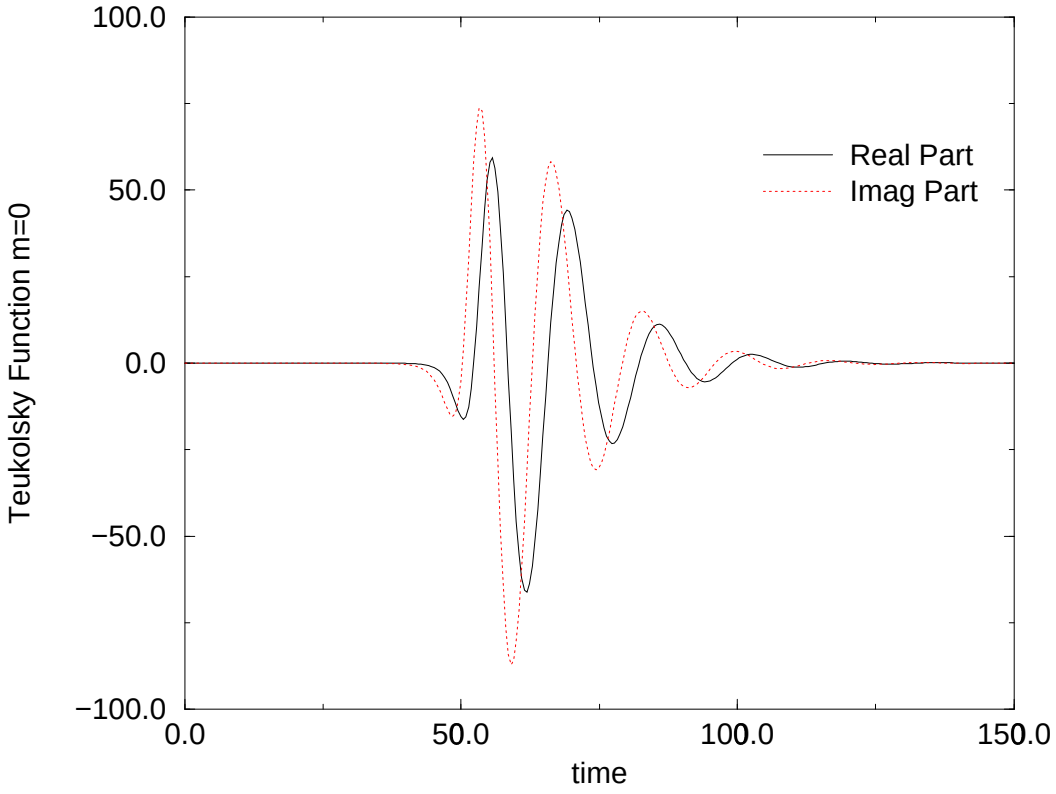

Fig. 3.1. This is the $m = 0$ mode of the Teukolsky function (Case I collision). The solid line depicts the real part whereas the dotted one, the imaginary part. All quantities are in units of ADM mass.

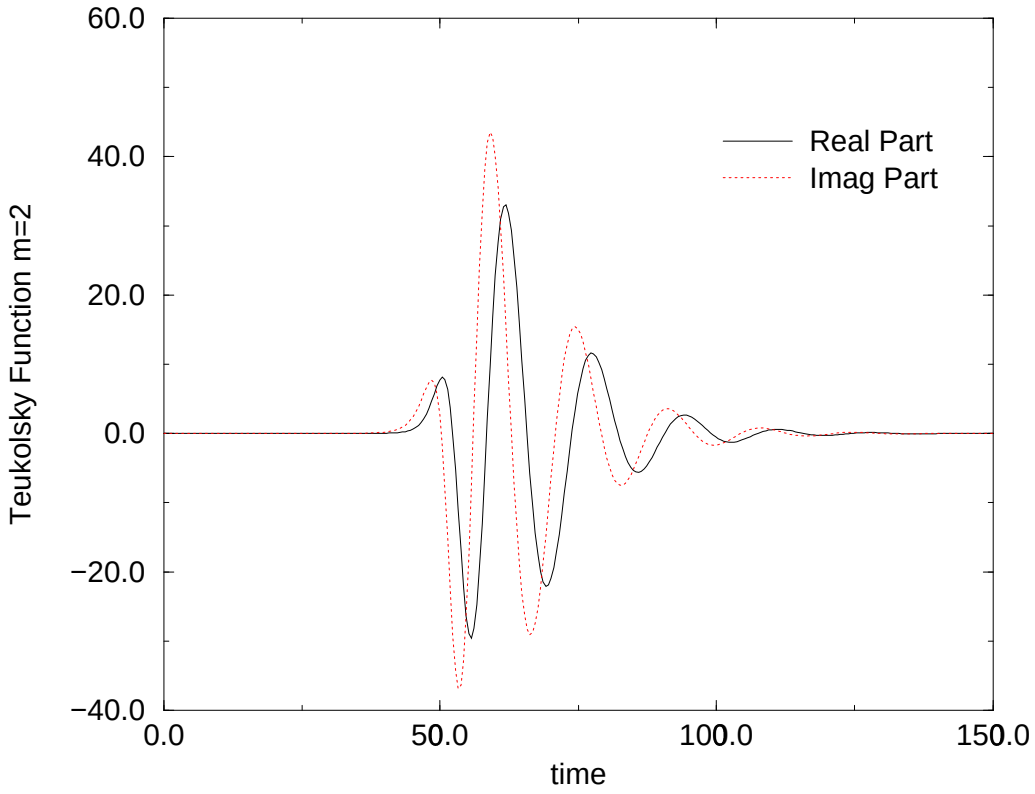

Fig. 3.2. This figure depicts the $m = 2$ mode of the Teukolsky function for a Case I collision. The solid line depicts the real part whereas the dotted one, the imaginary part. All quantities are in units of ADM mass.

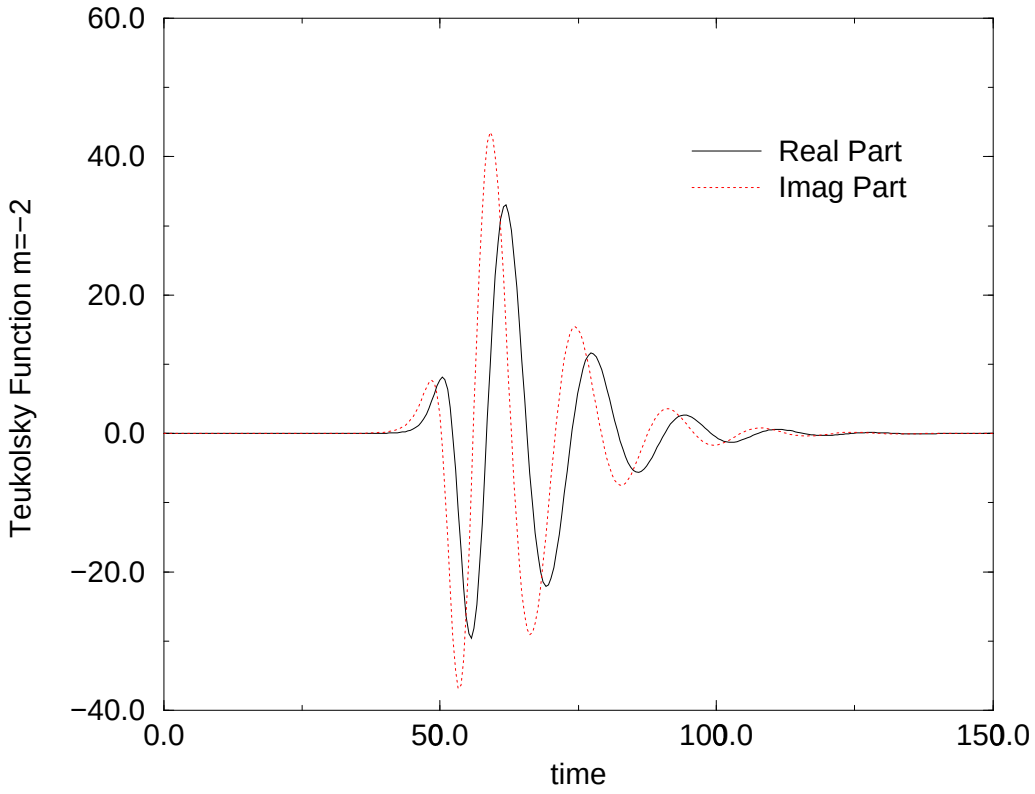

Fig. 3.3. This figure shows the $m = -2$ mode of the Teukolsky function for a Case I collision. The solid line depicts the real part whereas the dotted one, the imaginary part. All quantities are in units of ADM mass.

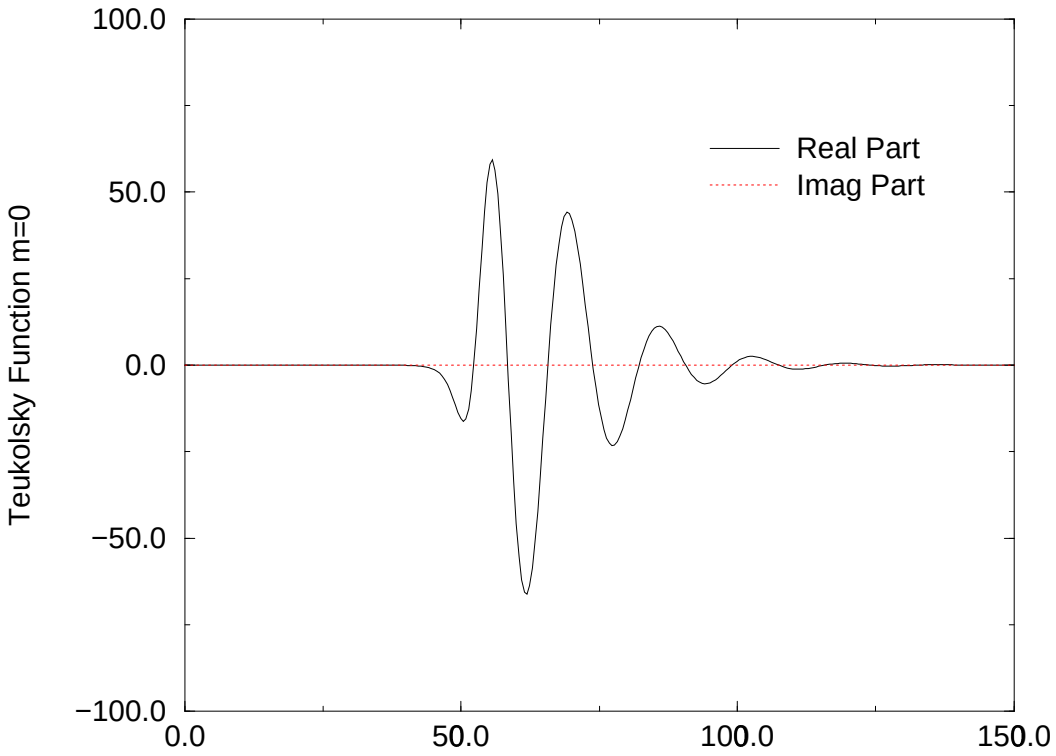

Fig. 3.4. This is the $m = 0$ mode of the Teukolsky function for a Case II collision. The solid line depicts the real part whereas the dotted one, the imaginary part. All quantities are in units of ADM mass.

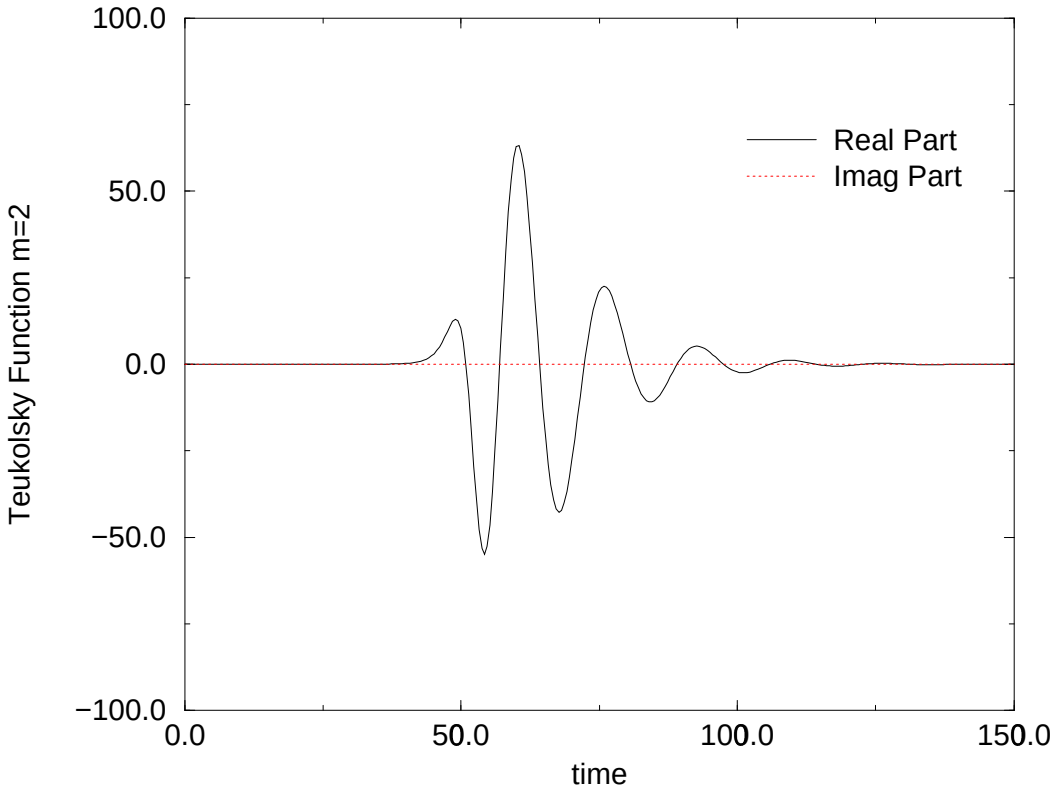

Fig. 3.5. This figure shows the $m = 2$ mode of the Teukolsky function for a Case II collision. The solid line depicts the real part whereas the dotted one, the imaginary part. All quantities are in units of ADM mass.

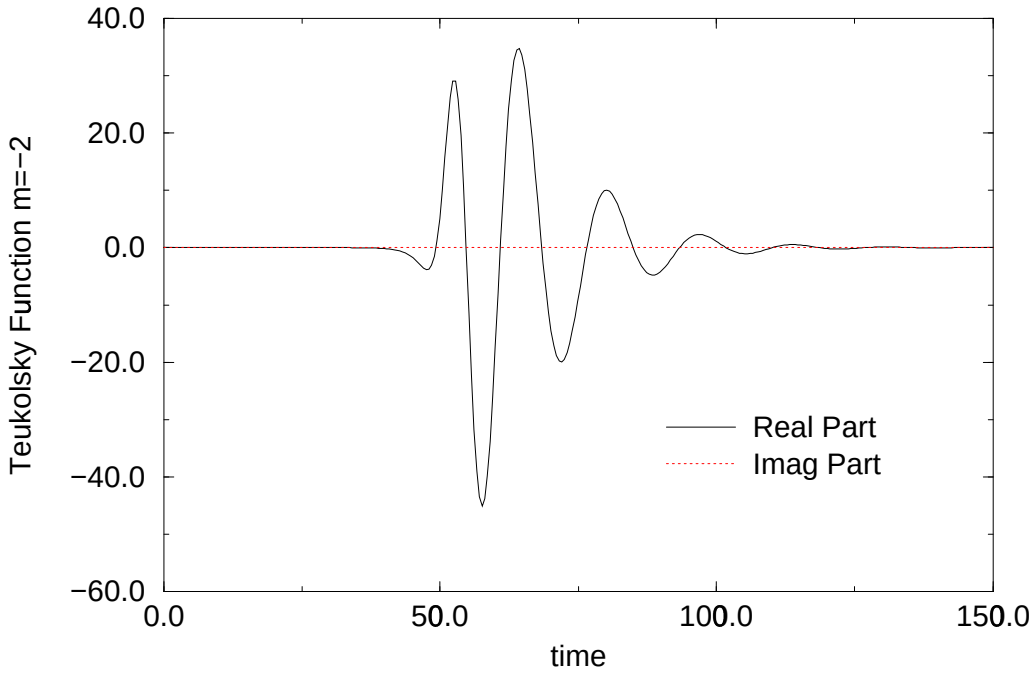

Fig. 3.6. This figure depicts the $m = -2$ mode of the Teukolsky function for a Case II collision. The solid line depicts the real part whereas the dotted one, the imaginary part. All quantities are in units of ADM mass.

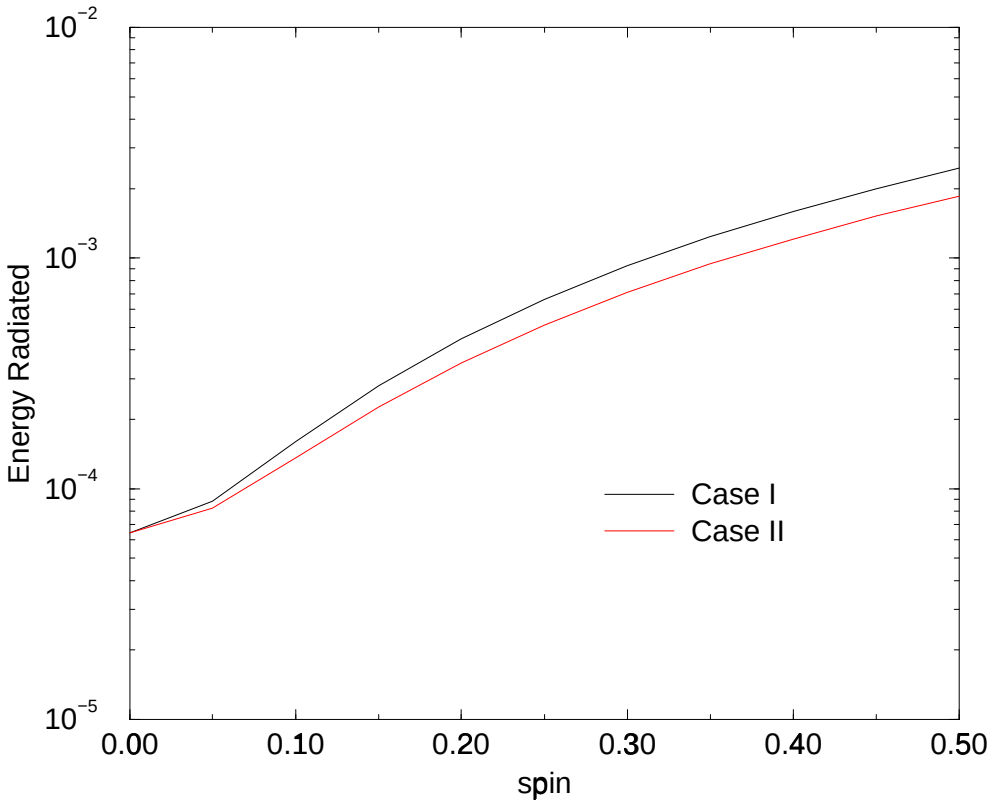

Fig. 3.7. The radiated energy in a head-on collision of two spinning black holes as a function of the individual initial spin (that is equal and opposite for the two holes), for a fixed conformal separation of 0.91. All quantities are in ADM mass units. Looking at the behavior of the curves for high spin, one can estimate that less than 1% of the mass of the system is lost in a typical collision involving spinning holes.

Chapter 4

Conclusions and future work

In this chapter we summarize our results and discuss possible future directions.

4.1 Conclusions

First, we used the "close limit" to estimate the radiation in the collision at the end of the inspiral of two equal mass nonrotating black holes. The assumptions and restrictions were: (i) only the "ringdown" radiation was computed; (ii) we assumed that a simple initial data set gave an adequate representation of appropriate astrophysical conditions; (iii) we assumed that the final hole is not near the extreme Kerr limit; (iv) we used close limit estimates of the evolution. Our main conclusion is that the energy radiated in ringdown is probably not more than 1% of the total mass of the system, and the angular momentum radiated is not more than 0.1% of the initial angular momentum.

Then we extended our calculations, to cover collisions of spinning holes. However, inclusion of spin did not change our original estimate of about 1% energy carried away by gravitational radiation in the late stage of black hole inspiral.

The most serious uncertainty in this result is the possibility that the radiation from the early merger stage of coalescence is very much larger than the ringdown radiation. With our $1\% Mc^2$ estimate, collisions of black holes of $100 M_\odot$ would be detectable

with signal to noise of 6 out to distances on the order of 200Mpc by the initial LIGO configuration and to distances of 4Gpc with the advanced LIGO detector [49].

4.2 Future directions

There are several avenues along which this work can be further developed. Firstly, its extremely crucial to do a comparision of these results with the limited, but full-nonlinear simulations that are currently available. Such a comparision will increase, tremendously, the confidence in techniques and methodology used for both types of calculations and results. One could also look into integrating the limited full-numerical simulations with the linear, stable perturbative evolutions in complementary way, and end up extracting a complete waveform! Another possibility, is to pursue this close limit inspiral problem, to higher order in perturbation theory. This will yield, much needed, limits and error bars for these first order results. And finally, the applicability of this close limit technique to other systems, like neutron star mergers etc. is in its infancy. A lot of work and ideas are needed there.

Appendix

The imposition of Cauchy data to the Teukolsky equation

Here we will answer the question of how to impose initial data to the Teukolsky equation (that describe perturbations around a rotating black hole). The work of reference [38] showed how to solve the problem for a nonrotating background, i.e. perturbations around a Schwarzschild hole by relating Weyl scalars ψ, to the Moncrief waveforms ϕ_M, an alternative description of metric perturbations explicitly built up out of the three-metric $\bar{g}_{ij}$ and the extrinsic curvature K_{ij} of the hypersurface $t =$ constant. In Ref. [40] the $\psi - \phi_M$ relations were successfully tested with a program for integration of the Teukolsky equation.

It is not obvious how to extend the above techniques to the rotating case. Thus, in the present work we turned to a more geometrical approach that lead us to the desired relations for *rotating* holes. In Sec. II we collect the results of the 3+1 decomposition reviewed in Ref. [41] relevant for our derivation. This has the advantage that makes ψ to be automatically independent of the shift, so our task is reduced to prove that terms depending on the first perturbative order lapse vanish. This is made in Sec. III, where we also build up $\partial_t \psi$ in terms only of $\bar{g}_{ij}$and K_{ij}. This results allow to compare, given the initial data, evolution through integration of the full Einstein equations and Teukolsky equation (linearization around a Kerr hole), and test, for instance, the close limit approximation for orbiting holes.

Notation: We use Ref. [42] conventions. An overbar on geometric quantities means that they are three-dimensional quantities, i.e. defined on the t = constant hypersurfaces Σ_t (an exception to this rule is the complex conjugation of the vector m^α, i.e. $\bar{\bar{m}}^\alpha$). (α,β) and $[\alpha,\beta]$ on indices α,β represent the usual symmetric and antisymmetric parts respectively. Greek letters indices run from 0 to 3 while latin letters indices run from 1 to 3. Subindexes (0) and (1) mean pieces of exclusively zeroth and first order respectively.

A.1 Geometric structure and gravitation

Following Ref. [41] we write the metric as

$$ds^2 = -N^2(\theta^0)^2 + g_{ij}\theta^i\theta^j, \tag{A.1}$$

with $\theta^0 = dt$ and $\theta^i = dx^i + N^i dt$, where N^i is the shift vector and N the lapse.

The cobasis θ^α satisfies

$$d\theta^\alpha = -\frac{1}{2}C^\alpha_{\beta\gamma}\theta^\beta \wedge \theta^\gamma \tag{A.2}$$

with $C^i_{0j} = -C^i_{j0} = \partial_j N^i$ and all other structure coefficients zero. Note that $\bar{g}_{ij} = g_{ij}$ and $\bar{g}^{ij} = g^{ij}$.

The spacetime connection one-forms are defined by

$$\omega^\alpha_{\beta\gamma} = \Gamma^\alpha_{\beta\gamma} + g^{\alpha\delta}C^\epsilon_{\delta(\beta}g_{\gamma)\epsilon} - \frac{1}{2}C^\alpha_{\beta\gamma} = \omega^\alpha_{(\beta\gamma)} + \omega^\alpha_{[\beta\gamma]}, \tag{A.3}$$

where $\Gamma^{\alpha}_{\beta\gamma}$ denotes the Christoffel symbol. These connection forms are written out explicitly in [43]. In particular, $\omega^{i}{}_{jk} = \Gamma^{i}{}_{jk} = \bar{\Gamma}^{i}{}_{jk}$, and the extrinsic curvature is given by

$$K_{ij} = -N\omega^{0}_{ij} \equiv -\frac{1}{2}N^{-1}\widehat{\partial}_0 g_{ij}, \tag{A.4}$$

where we define the operator

$$\widehat{\partial}_0 = \frac{\partial}{\partial t} - \mathcal{L}_{\mathbf{N}}, \tag{A.5}$$

with $\mathcal{L}_{\mathbf{N}}$ the Lie derivative on the hypersurface Σ_t with respect to the vector N^i. Note that $\widehat{\partial}_0$ and ∂_i commute.

The Riemann curvature tensor is given by[43]

$$R^{\alpha}{}_{\beta\rho\sigma} = \partial_\rho \omega^{\alpha}_{\beta\sigma} - \partial_\sigma \omega^{\alpha}{}_{\beta\rho} + \omega^{\alpha}{}_{\lambda\rho}\omega^{\lambda}{}_{\beta\sigma} - \omega^{\alpha}{}_{\lambda\sigma}\omega^{\lambda}{}_{\beta\rho} - \omega^{\alpha}{}_{\beta\lambda}C^{\lambda}{}_{\rho\sigma} \tag{A.6}$$

For rewriting in the next section the Weyl scalars in terms of hypersurface quantities only, we relate the spacetime Riemann tensor components to the 3-dimensional Riemann and the extrinsic curvature tensors

$$R_{ijkl} = \bar{R}_{ijkl} + 2K_{i[k}K_{l]j}, \tag{A.7}$$

$$R_{0ijk} = 2N\bar{\nabla}_{[j}K_{k]i}, \tag{A.8}$$

$$R_{0i0j} = N(\widehat{\partial}_0 K_{ij} + NK_{ip}K^{p}{}_{j} + \bar{\nabla}_i\bar{\nabla}_j N). \tag{A.9}$$

Another important relation in three dimensions is

$$\bar{R}_{ijkl} = 2g_{i[k}\bar{R}_{l]j} + 2g_{j[l}\bar{R}_{k]i} + \bar{R}g_{i[l}g_{k]j}. \tag{A.10}$$

The Ricci tensor $R_{\alpha\beta} = R^{\sigma}{}_{\alpha\sigma\beta}$ is given by

$$\begin{aligned} R_{ij} &= \bar{R}_{ij} - N^{-1}\widehat{\partial}_0 K_{ij} + KK_{ij} - 2K_{ip}K^{p}{}_{j} - N^{-1}\bar{\nabla}_i\bar{\nabla}_j N, & \text{(A.11)} \\ R_{0i} &= N\bar{\nabla}^j(Kg_{ij} - K_{ij}), & \text{(A.12)} \\ R_{00} &= N\,\bar{\nabla}^2\,N - N^2K_{pq}K^{pq} + N\widehat{\partial}_0 K. & \text{(A.13)} \end{aligned}$$

In order to incorporate the source terms we consider the Einstein equations as $R_{\alpha\beta} = T_{\alpha\beta} - \frac{1}{2}g_{\alpha\beta}T$. For instance, the "Energy constraint" is defined by

$$G^0{}_0 = \frac{1}{2}(K_{mk}K^{mk} - K^2 - \bar{R}) = T^0{}_0. \tag{A.14}$$

Finally, from its definitions

$$\widehat{\partial}_0\bar{R}_{ij} = \bar{\nabla}_k(\widehat{\partial}_0\bar{\Gamma}^k_{ij}) - \bar{\nabla}_j(\widehat{\partial}_0\bar{\Gamma}^k_{ik}), \tag{A.15}$$

where

$$\widehat{\partial}_0\bar{\Gamma}^k_{ij} = -2\bar{\nabla}_{(i}(NK_{j)}{}^{k}) + \bar{\nabla}^k(NK_{ij}). \tag{A.16}$$

Note that writing equations in terms of $\widehat{\partial}_0$ instead of ∂_t allowed us to get rid of the shift dependence. This is because $\widehat{\partial}_0$ is orthogonal to the spacelike hypersurface Σ_t.

A.2 Weyl scalars for Kerr perturbations

For the computation of gravitation radiation from astrophysical sources it is convenient to work with the Weyl scalar

$$\psi_4 = -C_{\alpha\beta\gamma\delta} n^\alpha \overline{m}^\beta n^\gamma \overline{m}^\delta,$$

since it is directly related to the outgoing gravitational waves. For perturbations around a Kerr hole we have

$$-\psi_4 = R_{ijkl} n^i \overline{m}^j n^k \overline{m}^l + 4R_{0jkl} n^{[0} \overline{m}^{j]} n^k \overline{m}^l + 4R_{0j0l} n^{[0} \overline{m}^{j]} n^{[0} \overline{m}^{l]}.$$

Eqs. (A.7) and (A.8) directly give us the two first terms in the above sum in terms of hypersurface geometrical objects (g_{ij}, K_{ij}). In the last term we have to make use of Einstein equation (A.11) to eliminate $\widehat{\partial}_0 K_{ij}$. If one now considers first order perturbations around a Kerr hole, one would have to consider in ψ_4 two types of terms: terms that involve first order perturbative Riemann tensors contracted with the background tetrads and terms that involve the Riemann tensor of the background contracted with three background and one perturbative tetrads. It is not difficult to see that the latter terms vanish for the Kerr background. For the Kerr geometry the only non-vanishing Weyl scalar is $\psi_2 = R_{\alpha\beta\gamma\delta} l^\alpha m^\beta n^\gamma \overline{m}^\delta$ and one can quickly see that the above contributions, even with one of the tetrads being a perturbative one, still vanish. For instance, consider the term $R_{ijkl0} n^i_{(1)} \overline{m}^j n^k \overline{m}^l$. This term vanishes because it is contracted with

two $\overline{m}$ vectors, and any contraction with a repeated tetrad vector of the Riemann tensor vanishes for the Kerr spacetime. Similar arguments apply to the other terms.

Let us turn our attention to the terms that involve the first order Riemann tensors contracted with the background tetrads. Taking a look at equations (A.7)-(A.9) we see that if one considers first order perturbations, we will have expressions involving the first order extrinsic curvature, metric, and lapse. We do not want our final expression to depend on the perturbative lapse. It is easy to see that it actually does not depend on it. For R_{0ijk} we see that the lapse appears as an overall factor. So the expression evaluated for the perturbative lapse is proportional to the expression evaluated in the background, which vanishes. For R_{0i0j} if we rewrite it using the Einstein equation (A.11) again the lapse appears as an overall factor and the same argument as for R_{0ijk} applies. As a separate check, we have verified the independence on the perturbative lapse and shift using computer algebra.

The final result for the first order expansion of the Weyl scalar ψ_4 therefore is,

$$
\begin{aligned}
-\psi_4 \;=\; & \left[\bar{R}_{ijkl} + 2K_{i[k}K_{l]j}\right]_{(1)} n^i \overline{m}^j n^k \overline{m}^l - 4N_{(0)} \left[K_{j[k,l]} + \bar{\Gamma}^p_{j[k}\, K_{l]p}\right]_{(1)} n^{[0}\overline{m}^{j]} n^k \overline{m}^l \\
& + 4N_{(0)}^2 \left[\bar{R}_{jl} - K_{jp}K^p_l + KK_{jl} - T_{jl} + \frac{1}{2} T g_{jl}\right]_{(1)} n^{[0}\overline{m}^{j]} n^{[0}\overline{m}^{l]}
\end{aligned}
\tag{A.17}
$$

where $N_{(0)} = (g^{tt}_{\rm kerr})^{-1/2}$ is the zeroth order lapse, $n^i, \overline{m}^j$ are two of the null vectors of the (zeroth order) tetrad (see Ref. [44]), latin indices run from 1 to 3, and the brackets are computed to only first order (zeroth order excluded).

To obtain $\partial_t \psi_4$, the other relevant quantity in order to start the integration of the Teukolsky equation, we can operate with $\widehat{\partial}_0$ on ψ_4 given by Eq. (A.17) to find

$$
\begin{aligned}
\partial_t \psi_4 &= N^{\phi}_{(0)} \partial_{\phi}\left(\psi_4\right) - n^{i}\overline{m}^{j} n^{k}\overline{m}^{l}\left[\widehat{\partial}_0 R_{ijkl}\right]_{(1)} \qquad \text{(A.18)}\\
&+4N_{(0)} n^{[0}\overline{m}^{j]} n^{k}\overline{m}^{l}\left[\widehat{\partial}_0 K_{j[k,l]} + \widehat{\partial}_0 \Gamma^{p}_{j[k} K_{l]p} + \bar{\Gamma}^{p}_{j[k}\,\widehat{\partial}_0 K_{l]p}\right]_{(1)}\\
&-4N^{2}_{(0)} n^{[0}\overline{m}^{j]} n^{[0}\overline{m}^{l]}\left[\widehat{\partial}_0\,\bar{R}_{jl} - 2K^{p}_{(l}\widehat{\partial}_0 K_{j)p} - 2N_{(0)} K_{jp} K^{p}_{q} K^{q}_{l}\right.\\
&\left.+K_{jl}\widehat{\partial}_0 K + K\,\widehat{\partial}_0 K_{jl} - \widehat{\partial}_0 T_{jl} + \frac{1}{2} g_{jl} T - N_{(0)} T K_{jl}\right]_{(1)}
\end{aligned}
$$

where we made use of the equality

$$
g_{ip}\widehat{\partial}_0 g^{pj} = 2N K^{j}_{i}.
$$

The derivatives appearing in Eq. (A.18) can be obtained from Eq. (A.13)

$$
\widehat{\partial}_0 K = N_{(0)} K_{pq} K^{pq} - \bar{\nabla}^{2}\, N_{(0)} - N^{-1}_{(0)} T_{00}, \qquad \text{(A.19)}
$$

from Eq. (A.14)

$$
\widehat{\partial}_0\,\bar{R} = 2K^{pq}\widehat{\partial}_0 K_{pq} + 4N_{(0)} K_{pq} K^{p}_{s} K^{sq} - 2K\,\widehat{\partial}_0 K - 2\widehat{\partial}_0 T^{0}_{0}, \qquad \text{(A.20)}
$$

and from Eqs. (A.10) and (A.4)

$$
\begin{aligned}
\widehat{\partial}_0 R_{ijkl} &= -4N_{(0)}\left\{K_{i[k}\,\bar{R}_{l]j} - K_{j[k}\,\bar{R}_{l]i} - \frac{1}{2}\,\bar{R}\left(K_{i[k} g_{l]j} - K_{j[k} g_{l]i}\right)\right\} \qquad \text{(A.21)}\\
&+2g_{i[k}\widehat{\partial}_0\,\bar{R}_{l]j} - 2g_{j[k}\widehat{\partial}_0\,\bar{R}_{l]i} - g_{i[k} g_{l]j}\widehat{\partial}_0\,\bar{R} + 2K_{i[k}\widehat{\partial}_0 K_{l]j} - 2K_{j[k}\widehat{\partial}_0 K_{l]i}.
\end{aligned}
$$

Note that in the last three equations we have taken explicitly the lapse to the zeroth perturbative order. This is so because in building up $\partial_t \psi_4$ explicitly all dependence on $N_{(1)}$ cancels out. To prove this one can do the explicit calculation for the Kerr background using computer algebra. An alternative is to notice that $\partial_0 \psi_4 = \mathcal{L}_t \psi_4$ where t^a is a vector that includes the background and first order perturbations of the lapse and shift. If one now expands out this expression one gets $\partial_0 \psi_4 = \mathcal{L}_{t_{(0)}} \psi_{4_{(0)}} + \mathcal{L}_{t_{(0)}} \psi_{4_{(1)}} + \mathcal{L}_{t_{(1)}} \psi_{4_{(0)}}$. Now, since $\psi_{4_{(0)}}$ vanishes identically for all time, the only contribution one has is $\partial_0 \psi_4 = \mathcal{L}_{t_{(0)}} \psi_{4_{(1)}}$. Therefore the time derivative of ψ_4 does not depend on the perturbative lapse and shift, since neither $\mathcal{L}_{t_{(0)}}$ (by construction) nor $\psi_{4_{(1)}}$ (due to the proof we gave above), do.

The other pieces needed to build up $\partial_t \psi_4$ only out of hypersurface data are $\widehat{\partial}_0 K_{ij}, \widehat{\partial}_0 \Gamma^k_{ij}$, and $\widehat{\partial}_0 \bar{R}_{ij}$ that are given by Eqs. (A.11), (A.16) and (A.15) respectively. As before, we have to consider the zeroth order lapse only, for instance

$$\widehat{\partial}_0 K_{ij} = N_{(0)} \left[\bar{R}_{ij} + K K_{ij} - 2 K_{ip} K^p{}_j - N^{-1}_{(0)} \bar{\nabla}_i \bar{\nabla}_j N_{(0)} - T_{ij} + \frac{1}{2} T g_{ij} \right]_{(1)} . \quad \text{(A.22)}$$

This completes our proof. A check of the relations (A.17) and (A.18) can be made in the Schwarzschild background for close limit initial data where [40] at t=0 we have $\partial_t \psi = -\frac{2M}{r^2} \psi$.

A.3 Discussion

The issue of expressing ψ explicitly in terms of hypersurface data only appears as of a purely technical character, but it is of great practical use. Especially when one thinks

of the important role played by first order perturbations as testbeds for comparison with full numerical integration of Einstein equations. Note that since Eqs. (A.17) and (A.18) hold on any $t =$ constant slice of the space time can not only be used to build up initial values for ψ and $\partial_t \psi$, but also at a later time to extract fully numerically generated wave forms.

The above equations provides the desired link between initial data (consisting of $\bar{g}_{ij}$and K_{ij}) and the Weyl scalar ψ_4. Geometrical objects like $\bar{\Gamma}^k_{ij}$, $\bar{R}_{ij}$ and $\bar{R}_{ijkl}$ involve first and second derivatives of the metric. Since astrophysical initial data for Kerr perturbations are numerically generated [45] this fact has to be taken into account. Expression (A.17) also includes a source term that allows to incorporate perturbations generated by particles or accretion disks around Kerr holes.

If one chooses to work in the Teukolsky equation with $\psi_0 = -C_{\alpha\beta\gamma\delta} l^\alpha m^\beta l^\gamma m^\delta$, which gives a better representation of ingoing gravitational waves, a completely analogous procedure applies to connect it to hypersurface data upon replacement of the double contractions with the corresponding null vectors l^α and m^β instead of n^α and $\overline{m}^\beta$.

Finally, we have been able to write ψ_4 and ψ_0 on the hypersurface Σ_t, but we did not said why. In fact it is not warranted that one can do that with any object defined on the spacetime. Is this because they are first order gauge invariant objects? This shouldn't be enough since we checked that for ψ_3 (and the same for ψ_1), we do not succeed in writing them in terms only of objects on the slice $t =$ constant. The key point here seems to be that ψ_4 and ψ_0 are also invariant under tetrad rotations and then directly connected to physical quantities, while ψ_3 and ψ_1 are not.

References

[1] See for instance, E. Seidel, in "Gravitation and relativity: At the turn of the millennium", N. Dadhich, J. Narlikar (eds.), Inter University Center for Astronomy and Astrophysics, Poona, India (1998).

[2] K. Schwarzschild, Sitz. Preuss. Akad. Wiss. 189 (1916).

[3] See P. Anninos, D. Hobill, E. Seidel, L. Smarr and W. Suen, Phys. Rev. **D52**, 2044 (1995) and references therein.

[4] For current information and links to all the interferometric gravitational wave detector projects see `http://www.ligo.caltech.edu`.

[5] For a recent discussion see S. Zwart, S. MacMillan, astro-ph/9910061, to appear in Ap. J. Lett.

[6] For a review on sources of gravitational waves see K. Thorne, gr-qc/9704042.

[7] For a review on post-Newtonian approximations see C. Will, Prog. Theor. Phys. Suppl. 136:158-167, 1999.

[8] A. Ptak, R. Griffiths, Astroph. J. **517**, L85 (1999); E. Colbert, R. Mushotzky, Astroph. J. **519**, 89 (1999).

[9] `http://lisa.jpl.nasa.gov`, `http://www.lisa.uni-hannover.de/`

[10] T. Regge and J. Wheeler, Phys. Rev. **108**, 1063 (1957).

[11] F. J. Zerilli, Phys. Rev. Lett. **24** 737 (1970).

[12] S. Teukolsky, Ap. J. **185**, 635 1973).

[13] M. Davis, R. Ruffini, W. Press, R. Price, Phys. Rev. Lett. **27**, 1466 (1971).

[14] See the discussion in E. Flanagan, S. Hughes, Phys. Rev. **D57**, 4535 (1997).

[15] For a recent review see J. Pullin, Prog. Theor. Phys. Suppl. 136:107-120, 1999.

[16] For a good discussion see the article by J. York in "Sources of gravitational radiation", L. Smarr (ed.), Cambridge.

[17] C. Misner, Phys. Rev. **118**, 1110 (1960).

[18] R. Price, J. Pullin, Phys. Rev. Lett. **72**, 3638 (1994).

[19] P. Anninos, R. Price, J. Pullin, E. Seidel, W.-M. Suen, Phys. Rev. **D52**, 4462 (1995).

[20] A. Abrahams, G. Cook, Phys. Rev. **D50**, 2364 (1994), see also J. Baker, C. B. Li, Class. Quant.Grav. **14** L77 (1997).

[21] R. Gleiser, C. Nicasio, R. Price, J. Pullin, Class. Quan. Grav. **13**, L117-L124 (1996); Phys. Rev. Lett **77**, 4483 (1996); Phys. Rev. **D59**, 044024 (1999); ref [30].

[22] J. Bowen, J. York, Phys. Rev. **D21**, 2047 (1980).

[23] B. Brügmann, S. Brandt, Phys. Rev. Lett. **78**, 3606-3609 (1997) .

[24] R. Gleiser, O. Nicasio, R. Price, J. Pullin, Phys. Rev. **57**, 3401 (1998).

[25] G. Cook, J. York, Phys. Rev. **D41**, 1077 (1990).

[26] D. Brill, R. Lindquist, Phys. Rev. **131**, 471 (1963).

[27] A.M. Abrahams and R.H. Price, Phys. Rev. **D53**, 1972 (1996).

[28] J. Baker, A. Abrahams, P. Anninos, S. Brandt, R. Price, J. Pullin and E. Seidel, Phys. Rev. **D55**, 829 (1997)

[29] F. J. Zerilli, Phys. Rev. **D2** 2141 (1970).

[30] R. Gleiser, C. Nicasio, R. Price, J. Pullin, Phys. Rep. 325:41-81, 2000.

[31] C. T. Cunningham, R. H. Price and V. Moncrief, Astrophys. J. **224**, 643 (1978); **230**, 870 (1979); **236**, 674 (1980); in *Sources of Gravitational Radiation*, ed. L. Smarr (Cambridge University Press, 1979).

[32] K.S. Thorne, Rev. Mod. Phys. **52**, 299 (1980).

[33] M. Campanelli, C.O. Lousto, J. Baker, G. Khanna and J. Pullin, Phys. Rev. **D58**, 084019 (1998)

[34] M. Campanelli, C. Lousto, Phys. Rev. **D59**, 124022 (1999).

[35] W. Krivan, P. Laguna, P. Papadopoulos and N. Andersson, Phys. Rev. **D56**, 3395 (1997).

[36] R. Gleiser, O. Nicasio, R. Price, J. Pullin, Phys. Rev. Lett. **77**, 4483 (1996).

[37] C.O. Nicasio, R.J. Gleiser, R.H. Price and J. Pullin, Phys. Rev. **D59**, 044024 (1999).

[38] M. Campanelli and C.O. Lousto, gr-qc/9711008.

[39] P. L. Chrzanowski, Phys. Rev. D **11**, 2042 (1975).

[40] M. Campanelli, W. Krivan and C. O. Lousto, gr-qc/9801067.

[41] A. Abrahams, A. Anderson, Y. Choquet-Bruhat and J. York Jr., Class. Q. Grav., **14**, A9-A22 (1997).

[42] C. W. Misner, K. S. Thorne and J. A. Wheeler, *Gravitation*, Freeman, San Francisco (1973).

[43] A. Anderson, Y. Choquet-Bruhat and J. York Jr., gr-qc/9710041.

[44] S. A. Teukolsky, Astrophys. J. **185**, 635 (1973).

[45] J. Baker and R. Puzio, gr-qc/9802006.

[46] W. Kinnersley , J. Math. Phys., **10**, 1195 (1969).

[47] H.-P. Nollert, J. Baker, R. Price, J. Pullin, gr-qc/9710011.

[48] J. Baker, Ph. D. thesis, Pennsylvania State University.

[49] J. Pullin, R. Price, private communication.

Vita

Gaurav Khanna was born in Chandigarh, India on March 30th, 1973. In 1995 he received a Bachelor of Technology degree in Electrical Engineering, from Indian Institute of Technology, Kanpur. The same year he enrolled in the doctorate program in Physics at the Pennsylvania State University. Throughout the program he was employed in the Physics Department of the Pennsylvania State University as a graduate assistant. For four years as a graduate student, Gaurav lived at different locations in State College, PA. In 1999 he married April A. Drumheller and moved to Sunbury, PA. After graduating in summer 2000, Gaurav joined Long Island University's Southampton campus as assistant professor.

Gaurav Khanna is a student member of the American Physical Society.